



HAL
open science

Adjustability of exposed elements by updating their capacity for resistance after a damaging event: application to an earthquake–tsunami cascade scenario

Caterina Negulescu, Abed Benaïchouche, Anne Lemoine, Sylvestre Le Roy, Rodrigo Pedreros

► To cite this version:

Caterina Negulescu, Abed Benaïchouche, Anne Lemoine, Sylvestre Le Roy, Rodrigo Pedreros. Adjustability of exposed elements by updating their capacity for resistance after a damaging event: application to an earthquake–tsunami cascade scenario. *Natural Hazards*, 2020, 104 (1), pp.753 - 793. 10.1007/s11069-020-04189-0 . hal-03742608

HAL Id: hal-03742608

<https://brgm.hal.science/hal-03742608>

Submitted on 2 Aug 2022

HAL is a multi-disciplinary open access archive for the deposit and dissemination of scientific research documents, whether they are published or not. The documents may come from teaching and research institutions in France or abroad, or from public or private research centers.

L'archive ouverte pluridisciplinaire **HAL**, est destinée au dépôt et à la diffusion de documents scientifiques de niveau recherche, publiés ou non, émanant des établissements d'enseignement et de recherche français ou étrangers, des laboratoires publics ou privés.



Adjustability of exposed elements by updating their capacity for resistance after a damaging event: application to an earthquake–tsunami cascade scenario

Caterina Negulescu, et al. *[full author details at the end of the article]*

Received: 26 February 2019 / Accepted: 16 July 2020 / Published online: 31 July 2020
© The Author(s) 2020

Abstract

The 2011 Great East Japan earthquake and tsunami remind us once again that these types of cascade event can occur and cause considerable damage. The scientific community realizes the need for rapid theoretical and practical progress on cascade events to provide field teams with the necessary tools and information for action during these types of events. The earthquake damage scenario for Martinique and Guadeloupe islands (French West Indies) has already been performed within the framework of French governmental projects, but these areas, in the vicinity of the French West Indies subduction zone, are also subject to tsunami events. In this study, we propose to perform a combined scenario in which an earthquake is followed by a tsunami, as it could arrive one day, considering the seismic characteristics and potential of such a subduction zone. The vulnerability of the buildings is defined considering local specific information based on several years of field inventories and inspections and is later classified into one of the 36 model building types of HAZUS. The calculation of the damages due to tsunamis follows the HAZUS methodologies. The main novelty of our study is the calculation of damage due to the two phenomena occurring one after the other, not in parallel, as is calculated in the existing literature. Therefore, for the calculation of the damages due to the second event (i.e. the tsunami), the vulnerability characteristics of the initial structure are reduced, considering the damage state of the construction after the first event (i.e. the earthquake). Hence, in our case, this calculation approach allows us to update the number of exposed elements and their changed vulnerabilities considering the damages due to the earthquake, since certain structures are already damaged by the earthquake before the arrival of the tsunami wave. The results coming from our study and our manner of treating the cascading hazards are putting into perspective with the Hazus method for combining damages coming from earthquake and the damages coming from consequently tsunami. The results expressed as the sum of the damages in both most damaged states, Extensive and Complete, are more or less in the same range of values for both studies (our study and HAZUS 2017). However, a trend of having more percentage of complete damages (and hence, less the Extensive damages) with our method than the ones obtained with the Hazus combination can be important information for crisis managing. This is a first result for the French West Indies territory, but anyway, more studies should be carried out in order to check this trend and eventually to confirm and validate this issue for others territories with others bathymetries, vulnerabilities and seismological features.

Keywords Tsunami flooding · Vulnerability adjustability · Cascading events · Combined earthquake–tsunami phenomenon · French West Indies

1 Introduction

Before addressing the question of the damages, due to the several quasi-simultaneous events, the methodologies for calculating the damage of each of these events should be developed and managed well. Next, the treatment of cascade effects from an event to other events and their interactions should be considered to give the most accurate prediction of the damage. The development of the methodologies for calculating the damage due to earthquakes started in the 1970s with the damage probability matrix of Whitman (Whitman et al. 1974) after the 1906 San Francisco Earthquake and currently continued to be improved. Based on this long experience, the methodology for performing the classic damage earthquake scenario is now well known, although each step of the methodology (e.g. shake maps, site effects, vulnerability assessments) can still be improved by, for example, the validation of the numerical results with the post-earthquake observed damage. A number of publications and software have been published and developed with this aim (e.g. GEM Technical Report Crowley et al. 2010a,b; Molina et al. 2010; Hancilar et al. 2010; FEMA 1999; FEMA 2004; Sedan et al. 2013).

Regarding the methodologies for calculating damages due to tsunami events, significant resources have been dedicated worldwide for improving hazard and damage models for tsunamis (Suppasri et al. 2015,2012) following recent large tsunamis (e.g. Murao and Nakazato 2010; Yamazaki and Cheung 2011 and Amakuni and Terazono 2011). More recently, the 2011 Tohoku earthquake tsunami in Japan has provided many data concerning structures (including engineered structures). Hence, the development of a fragility function for tsunamis increased after this event. There were 19 fragility functions derived by the data of this event compared to 11 fragility functions developed for all previous tsunamis combined (Charvet et al. 2017). Recent studies have tried to clarify or develop the different steps necessary to complete the methodology for damage estimations due to tsunami events, including the definitions of (1) the tsunami intensity measurement, (2) the inventory of the exposed elements and of their important characteristics, (3) typologies and their main characteristics and (4) the development or harmonization of the damage description. Park and Cox (2016) and Park et al. (2017) presented the probabilistic tsunami damage assessment and evaluated the influence of five intensity measures of tsunamis applied to Seaside, Oregon.

One of the most recent and complete studies that treat all these aspects was presented by Charvet et al. (2017), but several other previous studies are also very detailed and useful for understanding the main issues related to the tsunami damage scenario (Kircher and Bouabid 2014; Macabuag and Rossetto 2014; Tarbotton et al. 2015; Rehman and Cho 2016). Macabuag et al. (2016) went further in the details of analysis by correlating the damage degree distribution with the inundation depth distribution and building footprint distribution. Jaimes et al. (2016) proposed a new probabilistic tsunami risk assessment approach and exemplified it for public schools in southern Mexico. Browning and Thomas (2016) presented a method for determining an initial assessment of tsunami risk, with application for two coastal areas of Oman.

The work proposed in this paper addresses the *cascading effects* and interactions in the earthquake–tsunami damage scenarios (Fig. 1, right). With regard to the damage due to the quasi-simultaneous cascade events—in our case, an earthquake followed by a tsunami—not

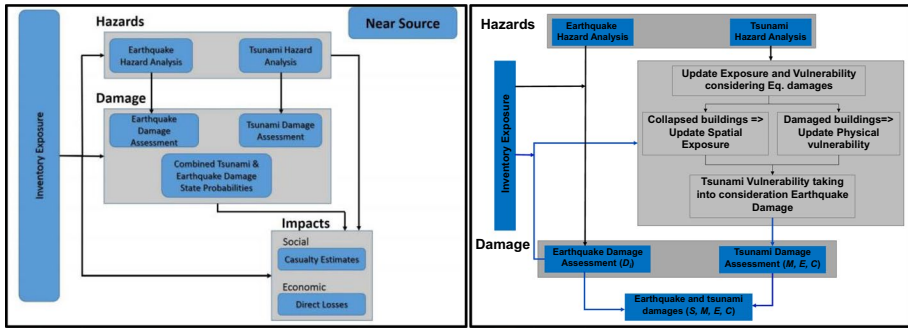


Fig. 1 Left: HAZUS Tsunami Model for Near Source Earthquake. Right: New developments (grey middle area and blue arrows) for considering combined cascade earthquake–tsunami damage assessment

many studies are available. When considering the combination of other phenomena, such as earthquakes, landslides or inundations, the SYNER-G (Systemic Seismic Vulnerability and Risk Analysis for Buildings, Lifeline Networks and Infrastructures Safety Gain, www.vce.at/SYNER-G) Project, funded by European Union’s Seventh Framework Programme (EU FP7), is a forerunner in the treatment of the combined events (Pitilakis et al. 2014). Of course, this topic of the damages due to the combined events has already been studied in the literature; however, the approaches used are more theoretical or propose a framework for how to consider the cascade or domino effects, and are rarely implemented in a software package or applied to a real case study, as is proposed in this paper. The Bayesian treatment of the cascading effects is modish and the advances proposed by this approach are valuable; however, most often they remain theoretical or applied only to network infrastructures. Gasparini and Garcia-Aristizabal (2014) discuss the role of the cascading effects triggered by the earthquake and its importance for a holistic view of the seismic risk assessment process. Mignan et al. (2016) treated the question of the cascading effects from the social point of view for assessing the adaptive capacities of the communities. The most representative studies that consider the damages both from the earthquake and from the induced tsunami are the paper related to the Great East Japan Earthquake (March 11th, 2011 Tohoku Earthquake). Considering the damage analysis and risk assessment, some studies are related to the 2004 tsunami in Phang Nga and Phuket, Thailand (Ruangrasamee et al. 2006; Rossetto et al. 2007; Römer et al. 2012). Nevertheless, these studies are either observation reports or retrospective questions related to prevention and mitigation measures (Epstein 2011). Generally, these studies treat the impact of the tsunami and the impact of the earthquake separately. Garcia-Aristizabal et al. (2015), within the EU FP7 CRISMA project (Modelling crisis management for improved action and preparedness, www.crismaproject.eu), implemented a concept model and tool for evaluating cascading effects into scenario-based analyses.

The scientific challenge comes from the fact that the tsunami-triggered earthquake is at the boundary of two specialties: the tsunami propagation is treated by fluid mechanics, and seismic faults and the building damages are treated by solid mechanics. Tsunami propagation is generally studied in the free field, and when the buildings are included, they are generally considered as non-deformable blocs or barriers, while in the case of the damage of buildings due to earthquakes, the buildings are deformable objects. Note that the terminology used to classify fragility functions, intensity measure or damage scale

can be different from one study to another for the same phenomenon (e.g. Tarbotton et al. 2015; GEM Crowley et al. 2010a, b; FEMA-HAZUS 1999; FEMA-HAZUS 2004; Prieto et al. 2018), and even more so when the phenomena are different. Tarbotton et al. (2015) reviewed the existing literature on tsunami fragility curves, noting trends and comparing existing fragility curves to highlight variability in the mean function across a range of studies. Charvet et al. (2017) presented a critical review and discussed the key issues in the current literature for each of the model components: building damage data, tsunami intensity data and the statistical model that links the two. They also presented a very complete table with the published empirical fragility functions for the 1993 Hokkaido-Nansei-Oki Tsunami, 2004 Indian Ocean Tsunami, 2009 Samoa Tsunami and 2010 Chilean Tsunami. As described in their table, the “Tsunami Intensity Measures” are numerous (h, inundation depth; v, velocity; F, drag force; MF, momentum flux; MMF, moment of momentum flux and FQS, a new proposed quasi-steady force estimate), and the number of the damage degrees can vary from 2 to 6. Generally, the fragility functions derived from data for the Great East Japan Earthquake and Tsunami use the damage scale proposed by the Japan Cabinet Office (2013). The equivalence or convergence of terminology from one study to another is a research topic in itself that will not be discussed in this paper. To overcome this debate, we chose to use the HAZUS guidance throughout this paper for characterizing the intensity measure, the building typologies and the damage scale, even if the software is conceived as such that, without any additional development, other terminologies can be applied in our research. The HAZUS (2017) choice is explained by the fact that earthquake and tsunami terminologies are self-consistent and by the fact that this document is the most recent one (November 2017), and can be considered as the most up-to-date development (Fig. 1, left). Kircher and Bouabid (2014) describe new functions for determining the probability of damage to buildings and essential facilities due to tsunami inundation (flood) and tsunami lateral force (flow) hazards, and for combining the damages due to these hazards with that due to earthquake shaking (i.e. for evaluation of damage and loss due to a local tsunami). The new building damage and loss functions were developed as part of a FEMA-funded project to develop a Tsunami Model for incorporation into the HAZUS Loss Estimation Technology. The Tsunami Model uses the same model building types, occupancy classes and building damage states as those of the Earthquake Model, descriptions of which may be found in the HAZUS technical manuals for earthquakes (FEMA-HAZUS 1999) and the Advanced Engineering Building Module (FEMA-HAZUS 2004). This version of HAZUS (HAZUS 2017) is able to run two types of damage analysis: both near-source (earthquake + tsunami) and distant-source (tsunami only). In this paper, we are interested in the combination of the earthquake and tsunami effects, called “near-source” analysis by HAZUS. Inputs to the calculation of tsunami damage to buildings include hazard data, namely, tsunami flood (inundation height) and tsunami flow (momentum flux), and earthquake damage data from the Earthquake Model (when evaluating local tsunami effects).

For the cascade event (i.e. earthquake followed by tsunami), we consider the simulated damage to structures due to the initial earthquake, and we return to the vulnerability function that we modify in order to consider the increase in its vulnerability regarding the damage degree achieved by the structure after the earthquake. In so doing, we consider this new increase vulnerability of the structure for the calculation of the tsunami damage. This is quite innovative for a scenario approach, and it is important to account for it for such near-source events, since there is likely to be increased vulnerability of some buildings to tsunami loading due to ground shaking, induced weakening of structures and the presence of loose debris that may be entrained in the tsunami flow (Fraser et al. 2014). Thus, the

exposed elements are updated after the damage seismic simulations, both in number and in the vulnerability characteristics. As in the HAZUS Tsunami Model from FEMA (2017), we combine earthquake and tsunami inventory attributes, and aggregate and analyse at the census block; however, the update of the exposed element is done by each typology in each census block. The census blocks used in our analysis were established after several years of field inventories (Bertil et al. 2009a; Roulle et al. 2010; Bertil et al. 2009b for Guadeloupe and Belvaux et al. 2013 for Martinique).

The Lesser Antilles arc is associated with the south-westward subduction of the North American plate under the Caribbean plate at a low convergence rate (i.e. 2 cm/year, DeMets et al. 2000). Moderate to large earthquakes can occur, related either to intraplate active faults or to the subduction process. Damaging historical events have been reported (e.g. SISFRANCE, BRGM 2018; SISFRANCE is the database of historical earthquakes felt in French territories). Moreover, the tsunamis of the French West Indies are mainly associated with regional earthquakes (e.g. Lambert and Terrier 2011), even if some teletsunamis (also called a transoceanic tsunami) were reported (e.g. Zahibo and Pelinovsky 2001; Lambert and Terrier 2011), in particular the tsunami induced by the great 1755 Lisbon earthquake. A teletsunami is a tsunami that originates from a faraway source, which is generally thousands of kilometres from the area of interest (Yu et al. 2011). In this study, we are paying attention to tsunamis induced by regional significant earthquakes. Two large destructive thrust interplate earthquakes occurred in the area: the 11 January 1839, east of Martinique Island, and the 8 February 1843, east of Guadeloupe Island (e.g. Bernard and Lambert 1988; Feuillet et al. 2011). Whereas these two damaging earthquakes, among the largest events reported in West Indies, are considered as reference events for seismic hazard analysis, their characteristics (i.e. magnitude, hypocentre or rupture description) still generate debates (e.g. Hough 2013). The 1843 earthquake is the largest known historical event associated with the Lesser Antilles subduction, contemporary testimonies give reports of intensity

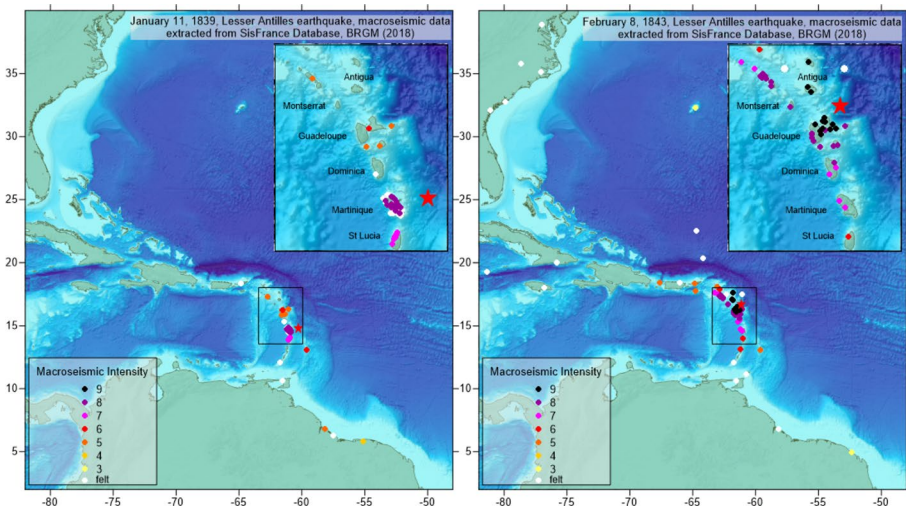


Fig. 2 Macroseismic intensity from SISFRANCE database and position of epicentres: for the 1843 earthquake west of Guadeloupe and for the 1839 earthquake west of Martinique. Red stars represent epicentre considered in this study (from Feuillet et al. 2011); bathymetry extracted from Gebco_2014 (Weatherall et al. 2015)

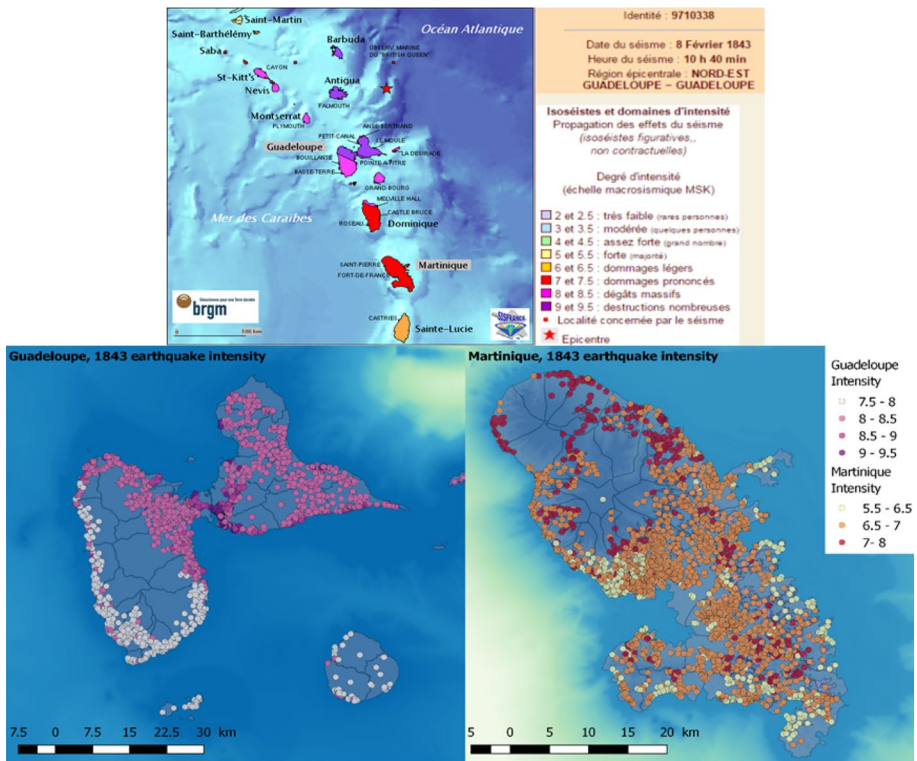


Fig. 3 Top—Macroseismic data from SISFRANCE database for 1843 earthquakes (https://www.sisfrance.net/Antilles/fiche_isoceiste.asp?NUMEVT=9710338) and bottom—intensities from Armagedom software simulations

IX (see Figs. 2 and 3), whereas only a moderate tsunami was reported (Bernard and Lambert 1988). In this case, it has been proposed for this event, from 7.5 to 8 (Bernard and Lambert 1988), to 8.5 or higher (Feuillet et al. 2011; Hough 2013). Whereas most of $M_w \geq 8.5$ megathrust earthquakes are associated with significant tsunamis, depending on source characteristics and on local conditions, some megathrust events were not associated with major tsunamis (e.g. Nias $M_w 8.6$ 2005 earthquake, Briggs et al. (2006). Le Roy et al. (2017) had used such hypothesis in order to model the moderate tsunami generated by the rupture of the deeper interface during 1843 earthquake. As the aim of the present study is not to analyse historical events, but to construct a realistic scenario for a cascade earthquake and tsunami damage estimation, source characteristics for 1843 and 1839 events proposed by Feuillet et al. (2011) were used. They proposed rupture along the subduction interface for the 1839 and 1843 events associated with $M_w 8$ and 8.5, respectively, and the source parameters they proposed generate significant near field tsunamis (see Table 1).

The main outcome of this study is the consideration of the earthquake damage that may precede tsunami damage and compromise building resistance, in case of near-source events. This is all the more important, especially for EQ-vulnerable buildings, as is the case in the French Lesser Antilles area. From a practical viewpoint, this implies the update of the exposed elements in the scenario, considering the damages due to

Table 1 Characteristic of the earthquakes

Scenario	M	depth (km)	Long. (°)	Lat. (°)	Fault type	Strike (°)	Dip (°)	Rate (°)	Length (km)	Width (km)	Slip (m)	GMPEs	Acc.-intensity conversion
IOG (Feuillet et al. 2011)	8.5	40	-61.17	16.73	Thrust (megathrust, dip 20°)	147	20	90	300	75	15	Youngs et al. (1997)	Atkinson and Somley (2000)
IOM (Feuillet et al. 2011)	8	30	-60.3	14.8	Thrust (megathrust, dip 20°)	160	20	90	140	50	8	Youngs et al. (1997)	Atkinson and Somley (2000)

the earthquake. Future studies should also assess tsunami risk to vital lifeline components, such as bridges and roads. Debris generated and casualty estimates also need to be investigated in future studies.

2 Co-seismic–tsunami cascade approach with exposure updating due to earthquake damages

Compared with the HAZUS methodology for near-source earthquakes, where the total damage occurs as the result of a combination of earthquake and tsunami hazards calculated separately without interaction (Fig. 1, left), our approach calculates the damages in one event after the other. This approach allows the updating of the exposed elements and especially their vulnerability, based on the damages caused by the earthquake, for the tsunami damage calculation (blue arrows in Fig. 1, right). This aspect is very important in the areas in which the earthquake vulnerability of structures is very low, as in our case study.

Considering the phenomenon as a cascade effect seems more realistic than treating each hazard separately and then proposing methods for combining the probability of building damage due to a tsunami with the probability of building damage due to the earthquake that generated the tsunami. Figure 1 (left) presents the HAZUS (2017) combined earthquake and tsunami methodology, and the alternative method proposed in this study (Fig. 1, right). Note that in the right side of Fig. 1, we propose to make a computation loop regarding the exposure, to update it considering the spatial distribution and to consider its new vulnerability established after the earthquake damage. Hence, this computation loop is applied to each census block, to each typology included in the census block and to each damage degree reached by each typology after the first event. The area of focus of the study is the French West Indies territory.

3 Seismic and tsunami hazard

3.1 Seismic hazard: source characteristics and intensity measures

Two earthquakes are considered: interplate earthquakes offshore Martinique and Guadeloupe (Fig. 2). Large historical events were reported in 1839 and 1843 offshore Martinique and Guadeloupe, respectively. Though they are generally associated with megathrust ruptures, no large tsunami were reported (e.g. Bernard and Lambert 1988 or Hough 2013). Nevertheless, source hypothesis from Feuillet et al. (2011) for these events are inspired from macroseismic data and active faults analysis. Both earthquakes are localized offshore, in the Atlantic Ocean, to the East of Martinique and Guadeloupe Islands. The epicentre of the 1843 earthquake is located to the west of Guadeloupe and the 1839 earthquake is located to the west of Martinique (Fig. 2). As explained in the lines hereby, when we are speaking about tsunami events, the 1843 earthquake is referred as IOG and the 1839 earthquake is referred as IOM. Such scenarios can be considered as “classical” scenarios for major rupture of the Lesser Antilles megathrust. These two scenarios are chosen better than others that could better explain that lack of significant tsunami in 1839 and 1843 as they represent an ideal case study for modelling near-source earthquake and tsunami damages. Moreover, even if such source characteristics fit macroseismic data and active faults characteristics, but did not fit tsunami data, they remain realistic hypothesis for rupture of

the Lesser Antilles megathrust offshore Martinique and Guadeloupe. Two hypotheses are considered for the damage assessment:

- A large mega thrust event offshore Guadeloupe from Feuillet et al. (2011), referred as Interplate Offshore Guadeloupe (IOG) scenario;
- A large thrust event offshore Martinique from Feuillet et al. (2011), referred as Interplate Offshore Martinique (IOM) scenario.

The localization of the two earthquakes is an important point for the interpretation of the results. Table 1 presents the parameters used for the generation of earthquakes.

The bedrock acceleration is calculated by a new developed python version of Armagedom software (Sedan et al. 2013 now integrated into VIGIRISKS platforme -Tellez-Arenas et al. 2019; Negulescu et al. 2019) using the fault position, the moment magnitude, the fault mechanism and the attenuation laws. The bedrock acceleration is majored with a soil coefficient to take into consideration the site effects that are quite important in this area. The site effects have been established during French Government projects that funded several years of H/V measurements and soil investigations first, for some communes (Bertil et al. 2009a; Roulle et al. 2010) and subsequently, for the entire territory (Sedan et al. 2008 for the methodology, Bertil et al. 2009b for Guadeloupe and Belvaux et al. 2013 for Martinique). Depending on the hazard intensity measure (IM) parameter used for the damage calculation (e.g. acceleration for HAZUS or EMS98 intensity for RISK-UE level 1 2001 – Milutinovic and Trendafiloski 2003), the acceleration can be converted to intensities. The calculation of the intensities for our simulations also provides the ability to check them with the historical information. Figure 3 compares the Armagedom simulation results in terms of intensities with that described by the SISFRANCE historical events database, which is an abundant and reliable database, and is the reference historical database in France (SISFRANCE, BRGM). Note that the range of intensities is quite similar for the Armagedom (Sedan et al. 2013) simulations and the historical data.

3.2 Tsunami hazard: propagation and submersion

To calculate the tsunami hazard parameter, which is the maximum moment flux, HAZUS uses the median value of the maximum inundation height, H (also called the water depth or flood depth, that is, the sea surface elevation minus the topography), and the median value of the maximum velocity of the water, v .

We use the inundation height grids and flow velocities grids calculated based on numerical simulations involving modelling the tsunami source, propagation and inundation. The tsunami hazard data include inundation grids provided from an external numerical tsunami hazard model (Le Roy et al. 2017; Poisson et al. 2009) that corresponds to a Level of Analysis 3 according to the HAZUS description. Tsunami generation is classically modelled with (Okada 1985) formulation. FUNWAVE-TVD (Shi et al. 2012) is applied in order to simulate tsunamis, solving the Boussinesq equations. Two chains of four nested ranks are prepared in order to be able to perform tsunami propagation and coastal flooding models for Guadeloupe and Martinique. Topo-bathymetric grids were built from different sources (Litto3D ©IGN-SHOM, HISTOLITT from SHOM and GEBCO). For finest rank, heterogeneous soil friction according to land use is used and obstacle to flood is integrated. In our study, the final grid mesh is in the range of 20 to 30 m. The inundation grids of the numerical tsunami hazard model give the height, H , and the velocity, v , of the water at each time step; thus, for each area there are 100 inundation grids by each intensity measure.

Generally, the maximum values of the height, H , and the velocity, v , of the water are not reached at the same step of the simulation in the same spatial cell. Hence, by looking separately to the evolution of the two parameters, the height, H , and the velocity, v , of the water, and by using their median values, some information could be lost and we could miss the highest moment flux ($H \cdot v^2$), which is the most important parameter for us, since the flux damages the structure. Hence, for the calculation of the tsunami hazard we decided to calculate the moment flux ($H \cdot v^2$) at each time step in each cell of the grid. Next, the hazard parameter that is compared with the building capacity is the maximum value of the moment flux for all time steps in each grid. Contrary to HAZUS, which uses the median value of the maximum height and velocity parameters, we use the real maximum moment flux, which is not reached at the same time in each pixel of the grid, as this clearly arrives in reality. Figure 4 presents the maximum sea surface elevation (SSE), around Pointe-à-Pitre in Guadeloupe and along Martinique coast for IOM-like and IOG-like events. Figure 4 presents the maximum sea surface elevation (SSE), around Pointe-à-Pitre in Guadeloupe and along Martinique coast for IOM-like and IOG-like events.

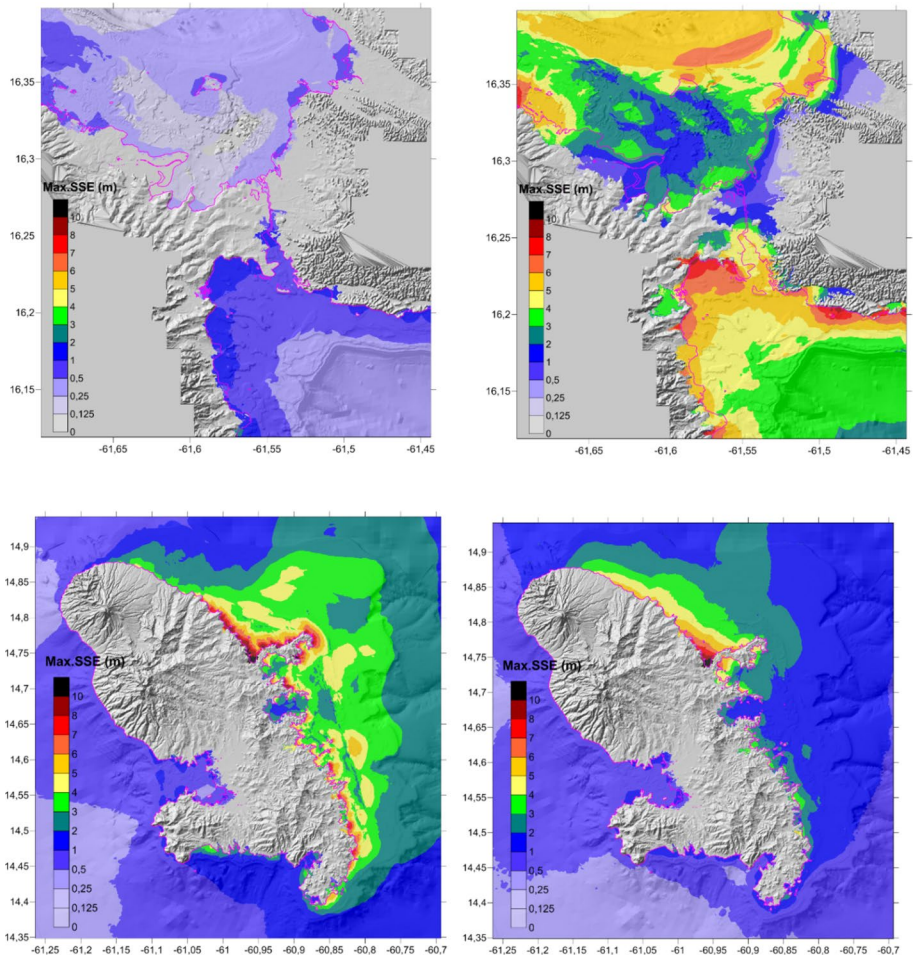


Fig. 4 Maximum sea surface elevation (SSE) around Pointe-à-Pitre (Guadeloupe, top) and Martinique (bottom) for IOM-like (left) and IOG-like (right) events. Tsunami hazard parameter maximum flood depth, H is then deduced (namely, sea surface elevation minus the topography). Initial coastline is in pink

4 Earthquake and tsunami inventory, vulnerability characteristics and damage calculation

The inventory of existing buildings was performed first by the GIS approach that determined the census blocks that could have the same vulnerability and occupancy characteristics. These census blocks are named “area of homogeneous vulnerability”. Second, field investigations by the teams of civil engineers of BRGM during a period of 5 years were conducted to validate or refine the “areas of homogeneous vulnerability”, called out further on the census block. These studies and field investigations were funded by different projects of the French Government, the same projects that characterized the soil characteristics. Bertil et al. (2009b) for Guadeloupe and Belvaux et al. (2013) for Martinique have finally regrouped these several projects. For some areas, extensive field inventories were performed; for others, extrapolations of the obtained data to the other communes were performed. The typologies were classified considering the local construction mode and local vulnerability aspects. Hence, the assessment of the vulnerability is based on local field inventories that took weeks to months to be performed, which corresponded to Level 2 of the HAZUS methodology. The total number of census blocks is 2950 for Martinique and 2054 for Guadeloupe. The spatial repartition of these census blocks is presented in Fig. 5. For each census block, the following information is provided: typologies, range of construction years, number of houses, number of dwellings, surface, density and type of occupation. In Fig. 5, we represented the density of each area classified as a function of the number of houses per hectare. The earthquake vulnerability is governed first by the earthquake-resistant design for both European and American approaches, and second by the construction material (wood, RC, masonry). In addition to the construction material, the assessment of the construction mode (e.g. cast-in-place, prefabricated) is also important. Finally, thanks to these data acquired during the French programmes, the buildings are classified in the 36 model building types of the HAZUS Tsunami Model, which are the same as those of the HAZUS Earthquake Model (FEMA 2011). For a coherence between the studies, we kept the “local name typologies” as a first column of Table 2 (named “Type CDRS”) and we observed the corresponding HAZUS Typologies and RISK-UE typologies. The double assessment of the vulnerability allows us to use, for the calculation of the buildings damages, either the RISK-UE or the HAZUS methodologies, or to use one

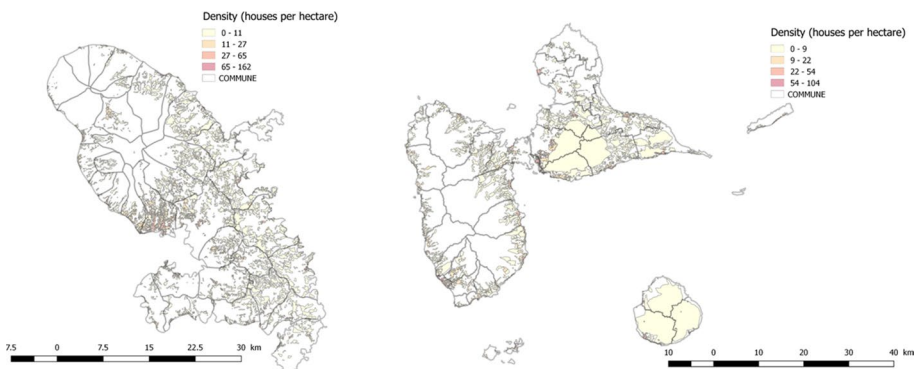


Fig. 5 Spatial repartition of the census blocks in Martinique (left) and Guadeloupe (right). The legend represents the density in houses per hectare

Table 2 Classification of the buildings in typologies

Type CDRS	RISK-UE type	HAZUS type	Seismic code	Structural type	Description	Main localization
Pierre	M1.1, M1.2	URMM	Pre-code	Unreinforced masonry bearing walls	Rubber stone, fieldstone, bad conservation	Downtown
Fortune	–	MH	Pre-code	Mobile homes	Assemblage of wood, sheet metal house, cement bloc	Area near downtown, suburbs
CaseTrad	W	W1	Pre-code	Wood, light frame (< 5000 sq. ft.)	Wood creole traditional building	Especially downtown
caseDur	W	W1	Pre-code	Wood, light frame (< 5000 sq. ft.)	Extension of a wood house either in wood either in unreinforced masonry, bad conservation	Especially downtown
VillaBois	W	W2	Medium	Wood, greater than 5,000 sq. ft	Wood timber individual building, good conservation	Suburbs, countryside
LotAnc	M3.4	URML	Pre-code	Unreinforced masonry bearing walls	One story, simply regular building, sometime auto-construction, masonry with manufactured stone units	Suburbs
LotRec	M4	RM2L	Medium	Reinforced masonry bearing walls with precast concrete Diaphragms	Respect CPM192 rules, regularity, bracing in both directions	Especially countryside
Pilotis Partiel	0.72	C3L	Pre-code	Concrete frame with unreinforced masonry infill walls	Mix of earthquake-resistant system: RC frame with infill masonry and reinforced masonry, total or partial transparency at ground level generally adapted to sloping ground, irregularities	Countryside
Pilotis R3R4	RC3.2	C3M	Pre-code	Concrete frame with unreinforced masonry infill walls	Mix of earthquake-resistant system: RC frame with infill masonry and reinforced masonry, total transparency at ground and first level, irregularities	Countryside

Table 2 (continued)

Type CDRS	RISK-UE type	HAZUS type	Seismic code	Structural type	Description	Main localization
Pilotis Total	RC3.2	C3H	Pre-code	Concrete frame with unreinforced masonry infill walls	Mix of earthquake-resistant system: RC frame with infill masonry and reinforced masonry, total transparency at ground level generally adapted to sloping ground, irregularities	Countryside
Villa R0R1	M4	RM1L	Low	Reinforced masonry bearing walls with wood or metal deck diaphragms	Simple, regular building	Downtown, suburbs, countryside
Villa R2R3	M4	RM1M	Low	Reinforced masonry bearing walls with wood or metal deck diaphragms	Simple, regular building	Downtown, suburbs, countryside
Villa Récente	M4	RM1L	Medium	Reinforced masonry bearing walls with wood or metal deck diaphragms	Respect CPMI92 rules, regularity, bracing in both directions	Especially countryside
ColAnc_L	RC3.2	PC2L	Pre-code	Precast concrete frames with concrete shear walls	Collective buildings constructed before 1975, no earthquake-resistant design, lack of bracing in a least one direction, often transparency at ground level	Suburbs
ColAnc_M	RC3.2	PC2M				
ColAnc_H	RC3.2	PC2H				
ColInt_L	RC2	C2L	Low	Concrete shear walls	Collective buildings constructed between 1976 and 1994, respect PS69 rules, moderate irregularities in plan, elevation and bracing	Suburbs
ColInt_M	RC2	C2M				
ColInt_H	RC2	C2H				
ColRec_L	RC2	C2L	Medium	Concrete shear walls	Collective buildings constructed after 1994, respect PS92 rules, some irregularities in plan and elevation	Suburbs
ColRec_M	RC2	C2M				
ColRec_H	RC2	C2H				

Table 2 (continued)

Type CDRS	RISK-UE type	HAZUS type	Seismic code	Structural type	Description	Main localization
ColVille AncR1R2	M4	RM2L	Low	Reinforced masonry bearing walls with precast concrete diaphragms	Contiguous building, commerce at ground level and apartment at superior levels	Downtown
ColVille AncR3R4	M4	RM2M	Pre-code	Reinforced masonry bearing walls with precast concrete diaphragms	Contiguous building, commerce at ground level and apartment at superior levels	Downtown
ColVilleRec	M4	RM2M	Medium			

method for the first event and another method for the second event, as a function of the approaches and the field data available. Table 2 details the typologies observed in the two islands, Martinique and Guadeloupe, and the classification following the model building type of the HAZUS Model and RISK-UE typology.

4.1 Earthquake and tsunami damage calculation

For the earthquake damage calculation, we can apply either the RISK-UE methodology, LM1 (empirical method) and LM2 (mechanical method) (Milutinovic and Trendafiloski 2003; Giovinazzi and Lagomarsino 2004), or the HAZUS methodology (FEMA 1999). Both of them are well known and are not detailed in this paper. Considering the historical database of intensities (SISFRANCE, BRGM), the field inventory data that we have and the experience acquired on the validation of the simulated damages with observed damages (Douglas et al. 2015; Boutaraa et al. 2018), we decided to apply RISK-UE methodology LM1 (the one based on relation between the intensity, the vulnerability index and beta damage distribution) for earthquake damage calculation. The decision to use RISK-UE methodology LM1 is also supported by studies made by others teams, for example Lestuzzi et al. (2016) that conclude that “There are significant differences in global results between LM1 (empirical method) and LM2 methods (mechanical method). The mechanical LM2 method is more pessimistic since it predicts damage grades of about one degree higher than LM1 method. However, the main drawback of the empirical LM1 method is that an a priori determination of an adequate value of the macroseismic intensity is required. Nevertheless, LM2 method may lead to a global overestimation of damage prediction”.

Regarding the tsunami damage calculation, the methodologies are less known, since they are quite recent. Several new approaches have been published lately (Attary et al. 2017; Petrone et al. 2017), and they generally use a Performance-Based Tsunami Engineering (PBTE) approach for tsunami damage assessments. This is also the approach adopted by HAZUS methodology (published in November 2017—FEMA 2017) and implemented in our study. Our research is focused on the structural damage; hence, we use the functions developed for tsunami “flow” hazard since the lateral forces due to tsunami flow are the primary cause of damage to the building structure, including building collapse. The damage due to tsunami inundation affects primarily the non-structural systems, which are not the object of our study and hence, the tsunami “flood” hazard is not considered in our scenario. More recently, Petrone et al. (2017) have compared tsunami pushovers to dynamic analysis in predicting structural responses, and they concluded that “tsunami peak force” is a more efficient intensity measure (IM) than flow velocity and inundation depth. This new parameter for tsunami intensity measure seems to have a good potential; however, its development is not sufficiently advanced nor sufficiently correlated with the other tsunami parameters (typologies, damage scale) to be integrated currently in general damage scenarios.

The damage on structures is due to the lateral forces caused by drag effects and debris carried along by the tsunami flow (Sect. 5.5 HAZUS Tsunami). The lateral force due to tsunami flow that acts on the structure is expressed by the following equation:

$$F_{TS} = K_d(0.5\rho_s C_d B(hv^2)) \quad (1)$$

where F_{TS} is the tsunami force on a building, K_d is a coefficient used to modify the basic hydrodynamic force, ρ_s is the density of the debris flow materials, C_d is the drag coefficient, B is the building plan dimension normal to the flow direction and hv^2 is the maximum momentum flux (flow depth times velocity squared).

The lateral capacity of a building is given by

$$F_y = \alpha_1 A_y W \text{ and } F_u = \alpha_1 A_u W \quad (2)$$

where F_y and F_u are the yield and ultimate force at the base of the building, respectively, α_1 is the modal mass parameter, A_y and A_u are the yield and ultimate spectral accelerations, respectively (Table 5.7 HAZUS EQ Technical Manual), and W is the total weight of the building.

By equating the debris flow force (Eq. 1) with the lateral building capacity (Eq. 2), we obtain the moment flux parameter, $h\nu^2$, for each damage state. The mean and median values of the building's strength, A_u and A_y , and their variabilities are taken from the HAZUS tables. The use of the lognormal damage probability functions is necessary to reflect the uncertainty. The metric for structural damage is the maximum flux as presented in Sect. 3.2. For the classification of typologies, for which we associated the A_y and A_u values, the building type and design level are important, as presented in Table 2.

At this stage, for the calculation of the tsunami damages, we do not consider the damages to structures due to the initial earthquake; in other words, all the structures have the initial vulnerability or are undamaged (damage state D0).

The influence of the debris of the collapsed buildings after the earthquake has not been accounted in Eq. 1. This issue is important and can affect the results but the estimation of this issue is complex and requires an important study in itself, that it is not in the scope of this paper. The debris of the collapsed buildings after the earthquake can have an important impact on the tsunami flooding in the damaged area and hence the risk of the first event can affect not only the vulnerability of structure, but also the extent of the hazard area of the second event. The debris of the collapsed buildings can change the soil roughness taken into consideration the flood extent estimation through the Manning coefficient. In this case, a better estimation of the tsunami flooding should be considered (up to high-resolution modelling) including an update of the Manning coefficient after earthquake damage calculation.

4.2 Earthquake and tsunami building damage states

For earthquakes, the two widely used damage scales in loss estimation studies are: (1) EMS-98 (Grunthal et al. 1998) an intensity (damage) scale developed primarily for post-earthquake field investigations; and (2) the US HAZUS (FEMA 1999) damage scale, an earthquake engineering scale from FEMA. These scales are used in both their original form and in a “hybrid” form (named by Hill and Rossetto (2008) “hybrid scales”—scales that are adapted versions of original scales). The RISK-UE project proposes scales for two methodology levels (Milutinovic and Trendafiloski 2003): LM1, based on post-earthquake field investigations and, hence, intensity parameters; and LM2, based on physical parameter values calibrated to European construction that follows similar principles to that used in HAZUS. In our software, both methodologies can be used. However, there is not a unique damage scale that can be used without interpretation and adaptation in the US and European context. This subject is difficult; for more detail the authors recommend the Hill and Rossetto (2008) study that carried out a complete review of damage scales for buildings with a view to assessing their suitability for use in earthquake loss modelling in Europe. They concluded that none of the considered damage scales adequately satisfies all the criteria necessary for their use in European seismic loss estimations, and consequently, they propose equivalence tables, showing the relationship between the damage states of each

considered scale. For earthquakes, the scales of damage that we are using in our simulations are RISK-UE (Milutinovic and Trendafiloski 2003) and US HAZUS (FEMA 1999).

For tsunamis, the building damage states are defined differently from one study to another and from one region to another. Among all the studies, three damage state definitions related to the tsunami as being the most adequate, the most used and therefore documented are (1) the Global Earthquake Model (GEM); (2) FEMA-HAZUS methodology; and (3) Japanese Ministry of Land Infrastructure Tourism and Transport. Eguchi et al. (2013) in their study, “HAZUS Tsunami Benchmarking, Validation and Calibration”, using the data after the 2011 Japan tsunami, mapped the damage states used in Japan into categories that are used by the HAZUS methodology (Fig. 6).

As our area of study is the French West Indies and the building characteristics are closer to the American structures than those constructed in Japan, we use the damage state definitions given by the HAZUS methodology. As shown in Table 3, three non-nil damage states are used for the tsunami by HAZUS: Moderate, Extensive and Complete. These damage states are the same as those (of the same name) used by the HAZUS Earthquake Model to describe the extent and severity of damage due to ground shaking and ground failure. Although the specific cause and manifestation of tsunami damage can be quite different from that of an earthquake, tsunami and earthquake damage states are considered to be the same when they represent a common extent and severity of damage (HAZUS 2017, 5.1.1).

The probability of occurrence of the complete damage is the value read on the corresponding fragility curve. The probability of occurrence of the extensive damage is the value read on the corresponding fragility curve minus the value read on the fragility curve corresponding to the complete damage state.

For clarity, and to separate the damages that come from the two phenomena, in Sect. 5 we address the damages from earthquakes in terms of the D0-D5 damage degrees (Column 3 of Table 3) and the damages from tsunamis in terms of Moderate, Extensive and Complete (Column 6 of Table 3). The damage coming from the combined earthquake–tsunami event is addressed in terms of Slight, Moderate, Extensive and Complete.

4.3 Update exposed elements and their vulnerabilities considering successive earthquake and tsunami aggression

The differences discussed in this section compared to the previous section are that we do consider the likely damage to structures due to the first event, the earthquake. Using the first hazard event and the initial vulnerabilities, we calculate the damage due to the first event. Then, we update the capacity of resistance to the lateral force for each typology in each census block taking into consideration the number of buildings in each typology that

Fig. 6 Mapping of Japanese damage descriptions to HAZUS damage states (after Eguchi et al. 2013)

Japanese Damage Level/State		HAZUS Damage State
1	Washed Away	Complete
2	Collapsed	
3	1 st Floor Inundation	Extensive
4	Major	
5	Moderate	Moderate
6	Slight	Slight/None
7	None	

Table 3 Definition of damage levels

Damage level	EMS98 Definition	RISK-UE (Milutinovic and Trendafiloski, 2003)		US HAZUS (FEMA 1999) Earthquake	US HAZUS (FEMA 1999; FEMA 2017) Tsunami
		LM1 EMS-based	LM2 HAZUS-based		
0	–	D0: No damage	None		
1	Slight damage, No SD, slight N-SD	D1: Slight	Minor		
				Slight	
2	Moderate damage, Slight SD, moderate N-SD	D2: Moderate	Moderate	Moderate	Moderate
3	Substantial to heavy damage, Moderate SD, heavy N-SD	D3: Substantial to heavy	Severe	Extensive	Extensive
4	Very heavy damage, Heavy SD, very heavy N-SD	D4: Very heavy	Collapse		
5	Destruction, Very heavy SD	D5: Destruction		Complete	Complete

SD is Structural Damage; N-SD is Non-Structural Damage.

SD is structural damage; N-SD is non-structural damage

reached each damage state (D0 to D5). Finally, we calculate the second event damages, based on the second hazard event and on the reduced vulnerability. The parameters that characterize the vulnerability of the structure were adapted (diminished) in order to consider the earthquake damage. In the calculations, we update two elements of the processes: (1) the number of the exposed element already damaged by the earthquake and (2) their vulnerabilities considering the impact of the earthquake.

For the exposed elements, we assume that the buildings that reached the damage degrees D4 and D5 after the earthquake no longer exist as exposed elements for the tsunami hazard, which comes after the earthquake damages. Hence, the first update is the total number of buildings by typology and by census block, considering the damage degrees caused by the earthquake.

Considering the vulnerability adaptability for the structures that are no damage, D0, or in damage degree D1, the tsunami method is applied without changing the vulnerabilities. For the buildings in damage degrees D2 and D3, the initial method presented in Sect. 4.2 is modified to consider that the structure is not in its original state, but is already damaged. That means the modification at the level of the yield and ultimate spectral acceleration (A_y and A_u) parameters. Figure 7 shows the initial capacity curve of the structure and the points green, yellow, orange and red that represent the spectral displacement when the corresponding damage state is reached. At the same time in Fig. 7, we represent in the colours green and orange the reduction in the rigidity of the structure, through the inclination/angle of the elastic branch of the capacity curve, after reaching a certain damage degree. As an example, in the top right part of Fig. 7, we are showing a real case of four identical buildings for which we performed microtremor measurements and analysis after the 2007 Martinique earthquake. The measured frequencies follow the reduction in the rigidity of the structures due to the damages occurred; the damages are different from one structure to another. The red, orange and green colours of this table can be associated, for an exemplification aim, with the red, orange and green points of the capacity curve. In order to apply a general approach for all the structures, to compute the residual capacity of a mainshock-damaged building to withstand an aftershock (or another lateral solicitation as is the case

of the tsunami flow) we used the tool SPO2IDA (Vamvatsikos and Allin Cornell 2006). SPO2IDA provides a direct connection between the static pushover (SPO) curve and the results of incremental dynamic analysis (IDA).

Therefore, for the purpose of calculating the A_y and A_u parameters for the building that already reached a certain limit state, LS_i , we use a practical tool called SPO2IDA, which is capable of converting static pushover curves into 16%, 50% and 84% IDA curves using empirical relationships from a large database of incremental dynamic analysis results. Hence, using SPO2IDA, we recreate the seismic behaviour of oscillators with complex quadrilinear backbones and different rigidity inclines to simulate a building that has already reached a certain LS_i . From Luco et al. (2004) in Fig. 8 (left), there is a representation of a pushover curve for an undamaged structure (D0); Fig. 8 (right) shows the “reduced” pushover curves considering the limit state, LS , reached by the structure after the first event.

Hence, from a development viewpoint, the initial file that describes the vulnerability is replaced by six files of vulnerability to have the new parameters that characterize the structure that reached each one of the damage states (D0 to D5) after the main shock. To implement this procedure in a more general process of a damage scenario, this procedure is integrated and implemented in the software for each typology and for each census block, as described in Fig. 9.

Of course, each of these two processes can be perfected. The aim here is neither to debate what reference to choose for one or another coefficient, nor to have an exhaustive view of these values, but to apply to the scenario process all these updates, and to evaluate for the chosen values the impact on the total damage. In this case, the aim is to apply the informatics and physical processes, and not to test one or another coefficient.

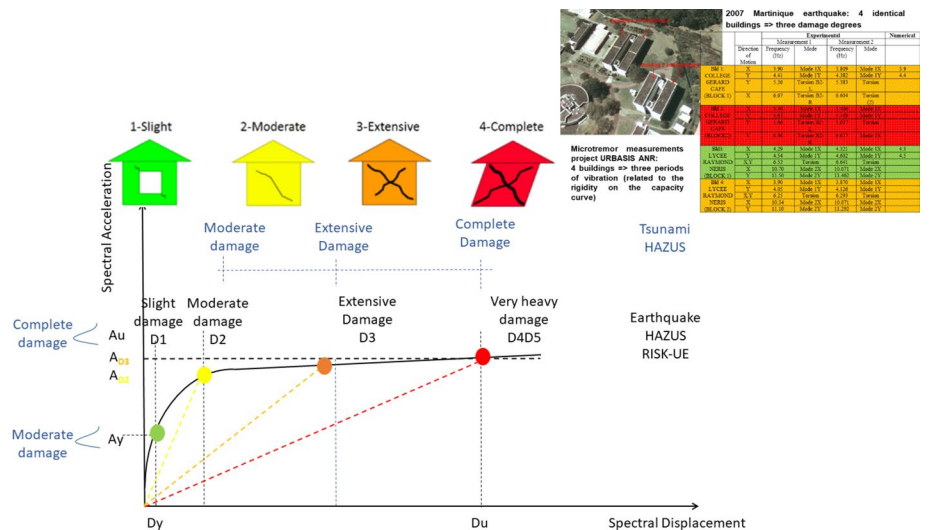


Fig. 7 Update of vulnerability properties for the already damaged structures (adapted from FEMA-HAZUS 1999)

5 Damage calculation for independent events and for successive earthquake–tsunami cascade events

5.1 Earthquake scenario

The main work in this paper is related to the tsunami and cascade damage calculation, and hence, the descriptions of the damages due to earthquakes are not highly detailed. Naturally, a good estimation of the earthquake damage is essential for a reliable treatment of results thereafter. Hence, we here present the results for the entire islands (Figs. 10, 11) and for the zoomed areas, respectively, corresponding to the area that is most affected by the tsunami in each one of the two islands: Trinity in Martinique and Pointe-à-Pitre in Guadeloupe. Further attention is paid to these zoomed areas. Figure 10 presents the results for the 1839 earthquake in Martinique, where we note that the Eastern part of the island is more affected than the Western part. This is normal considering the epicentre position of the earthquake (Fig. 2, left) added to some digital elevation model (DEM) characteristics leading to local tsunami amplification (e.g. La Trinité to the west of Martinique). Hence, Fort-de-France is not much impacted by the earthquake and tsunami, contrary to the east of the Island where the percentages of the damage degrees D4 and D5 reached 30% in a census block.

Hence, Fort-de-France is not much impacted by the earthquake and tsunami, contrary to the east of the Island where the percentages of the damage degrees D4 and D5 reached 30% in a census block. The high rate of damage coming from the earthquake event considerably affected the results on the combined cascade event. Figure 11 presents the earthquake damages in Guadeloupe for the 1843 earthquake, which was more damaged than in 1839 in this island. The percentage of damage degrees D4 and D5 can reach up to 50% in some census blocks. Even though the epicentral position is located in Northeast of Guadeloupe (Fig. 2, right), the area of the Pointe-à-Pitre Bay is largely affected by both earthquake and tsunami events.

For the More Classical Scenario for 1843 (or IOG-like), Fig. 12 shows a bigger damage degree for Guadeloupe since the damage distribution is centred on D2 (Guadeloupe is closest from the epicentre of 1843 event), while for Martinique the damage distribution is centred on D0. Inversely, the IOM-like earthquake damage is more important in Martinique centred in D2 (closest to the 1839 epicentre), while for Guadeloupe the large majority of buildings are undamaged (damage degree D0). As outlined in Chapter 3, Seismic

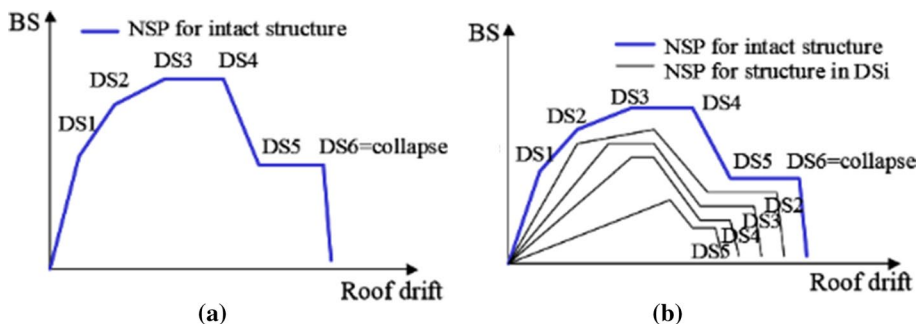


Fig. 8 Intact pushover curve and pushover curve for structures in a certain limit state, LS_i (from Luco et al. 2004)

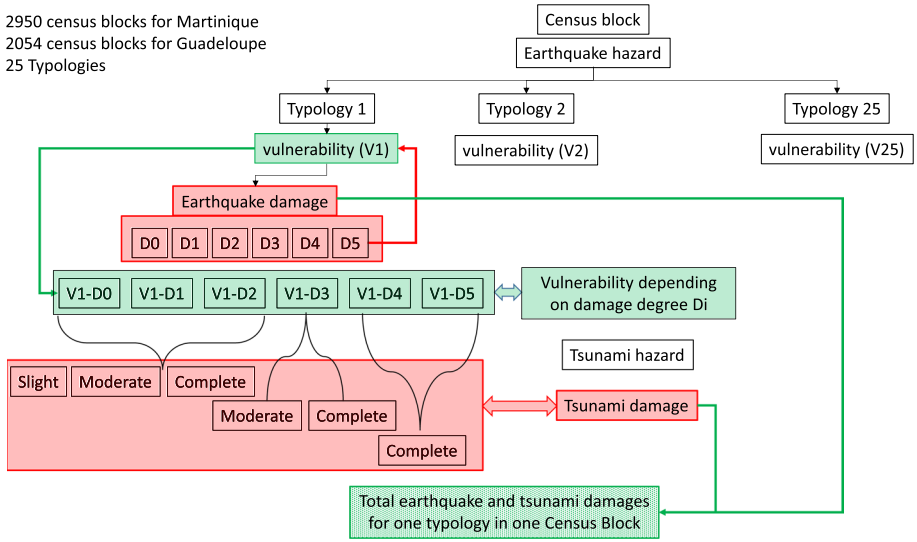


Fig. 9 Implementation of the vulnerability update, for each typology in each census block, considering the LSi reached after the first event

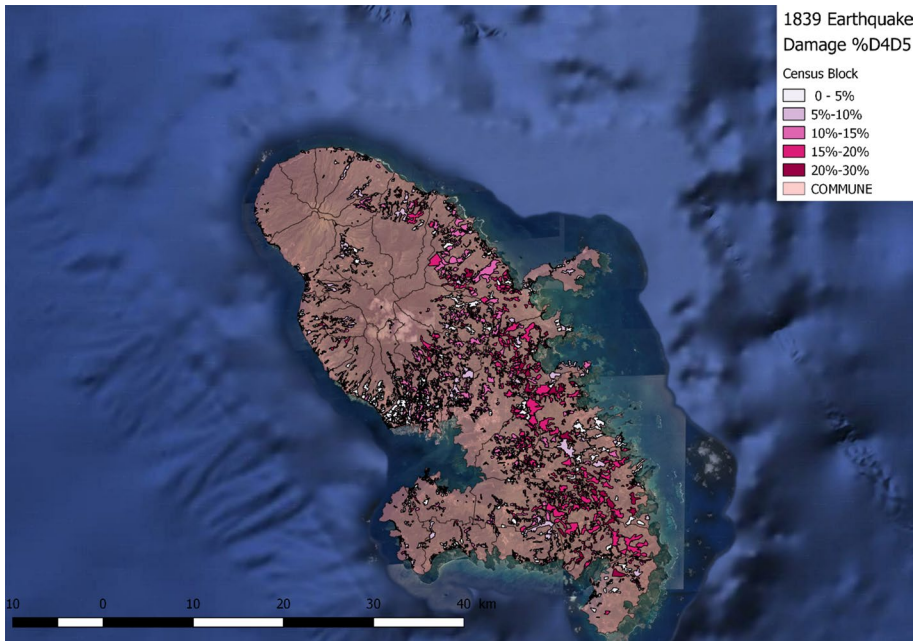


Fig. 10: 1839 Martinique earthquake (IOM-like) damage: percentage of damage degrees D4 and D5 per census block

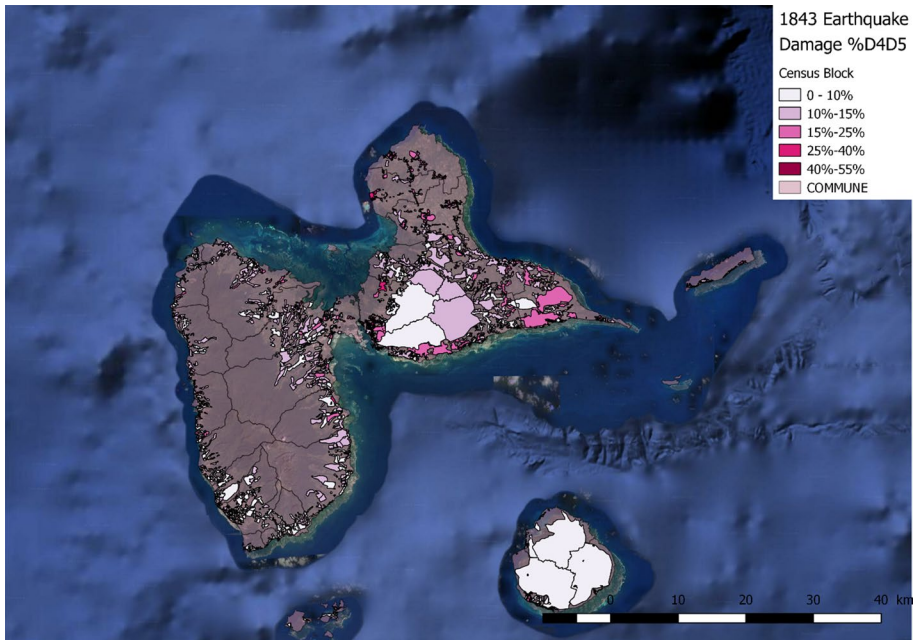


Fig. 11: 1843 Guadeloupe earthquake (IOG-like) damage: percentage of damage degree D4 and D5 per census block

and Tsunami Hazards, the historical observations of the intensities confirm the simulated seismic intensities (Fig. 3); hence, when we are speaking about the earthquake events the 1843 and 1839 earthquake can be mentioned like this, since they provoked these intensities. However, the historic data cannot sustain a hypothesis of a significant tsunami with the value modelled in our study; so, in this case we refer rather to IOG-like event than to the 1843 earthquake and, respectively, to IOM-like event than to the 1839 earthquake.

5.1.1 Tsunami scenario and cascade event earthquake–tsunami scenario

The difficulty of combining or comparing the damages coming from different events stems also from the difference of the scale of the impacted areas. The earthquakes, situated in the sea at East of either Guadeloupe or Martinique, affect both entire islands, in a greater or lesser degree of damage. Hence, in the case of earthquakes, the scale of the treatment of the damage is the scale of the entire Islands. The tsunami flooding maps show that for both earthquakes, the areas affected by the generated tsunamis are quite localized. For Guadeloupe, the area most affected by the tsunami coincides with the densest area in the Bay of Pointe-à-Pitre. Figure 13 shows the impact of the tsunami that affected the bay, described in terms of the intensity measure by the momentum flux. The amplification of the tsunami waves is certainly due to bathymetry and to the geographical configuration of the bay, with the coasts relatively close where tsunami wave rushes. In the legend of Fig. 13, we present the inundation height and the momentum flux, which take also in account the water velocity. This explains why, we can observe, for almost the same value of inundation height, different range of values for the moment flux represented at the scale of census blocks. For

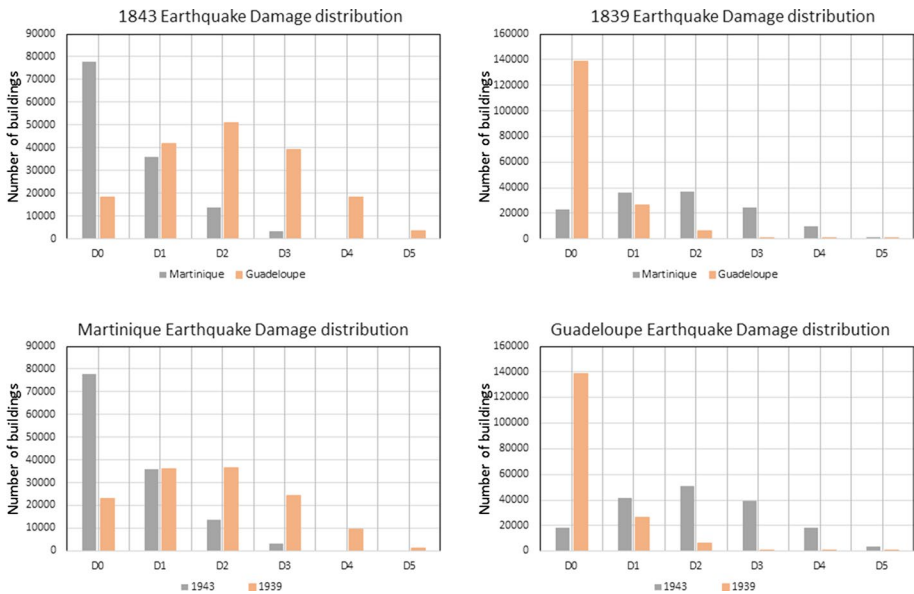


Fig. 12 Comparison between Martinique and Guadeloupe earthquake damage distribution for 1843 Guadeloupe earthquake (IOG-like) and 1839 Martinique earthquake (IOM-like)

example, in the left hand of Fig. 13, for an inundation height of around 3 m, we have one census block in the moment flux range between around 20 and 30, and the other neighbour census blocks in the moment flux range between around 10 to 20. For a better understanding, in order to discuss the results of tsunamis, we present here the figures zoomed in on the tsunami affected areas: Trinity in Martinique and Pointe-à-Pitre in Guadeloupe. To exemplify the difference of scale of the affected area by the earthquake and tsunami, Figs. 14 and 15 present the damages from the IOG-like tsunami and the damages from the IOG-like earthquake at the area of Pointe-à-Pitre Bay, respectively.

Note that the area impacted by the tsunami is contiguous to the coast line, while for the earthquake, it is spread throughout the entire island. This is an obvious observation from a phenomenological viewpoint; however, this observation alerts us as to how combining the damages coming from the cascade events that do not have the same impact scale. Figure 16 quantifies this localization of damage for the tsunami by comparing the damages for all islands and for the impacted areas by tsunami for the IOG-like tsunami. The bottom illustrations of Fig. 16 show that there is practically no difference of damage between all of Guadeloupe and the Bay of Pointe-à-Pitre, and hence, all the tsunami damage is concentrated in a very small territory. Concerning Martinique, there is a more important difference in the damages for all of Martinique and the Trinity damages, especially for the complete damage, which indicates that some other costal communes were affected by the IOG-like tsunami.

Figure 17 shows the distribution of damages for the IOM-like tsunami. Guadeloupe has not been impacted (see Fig. 17 right). Concerning Martinique, as for the IOG-like tsunami, we note that a large amount of damage is concentrated in Trinity. In Trinity, for the IOM-like and IOG-like tsunamis, we observe almost the same damage distribution; certainly, the same area is impacted. For the entire Martinique Island, the number of damaged

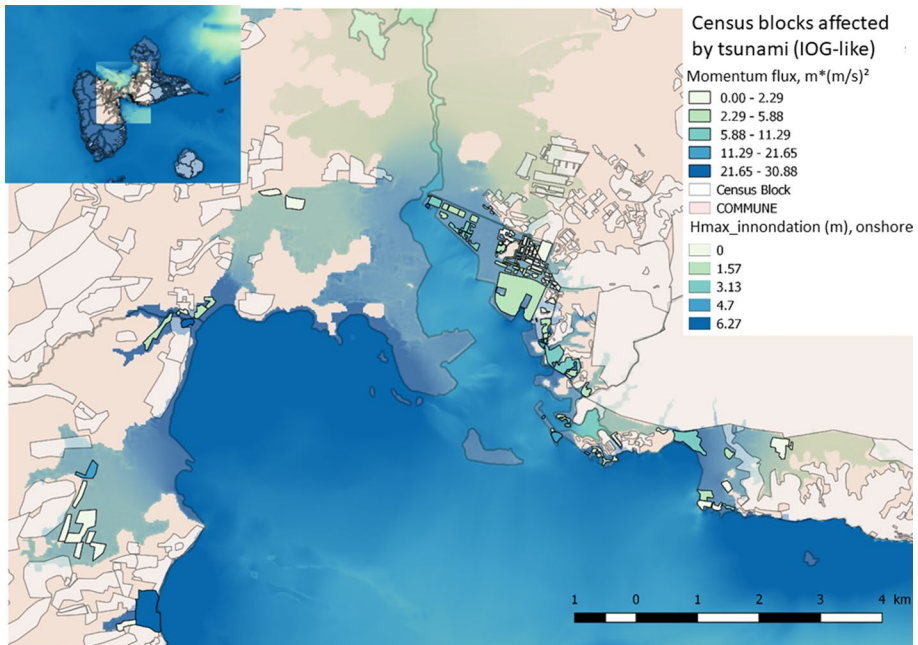


Fig. 13 Tsunami affecting Pointe-à-Pitre Bay: intensity measure described by the momentum flux

habitations increased from approximately 270 completely damaged structures for IOG-like event (chart bottom left of Fig. 16) to approximately 450 for IOM-like (chart left of Fig. 17).

Keeping in mind Fig. 14 (only tsunami event) and 15 (only earthquake event), Fig. 18 compares to themes, the damage at the scale of Pointe-à-Pitre coming from the combined cascade event—the earthquake and tsunami. We note that the majority of the areas affected by the tsunami in one category of damage (e.g. 0–10%, 10–35%) make a jump in the higher category of damage when we consider the cascade event. This is the case for the central area of Fig. 18, already affected by the tsunami and now almost completely damaged after the cascade event. For the bottom areas, right and left, of Fig. 18, we also note that some areas that seem to not have complete damage state neither after tsunami nor after the earthquake, present finally complete damage state after the cascade event.

Zooming in on Trinity, Martinique, Figs. 19, 20 and 21 show the damages due to the earthquake, tsunami and combined event earthquake, and tsunami for the IOM-like event, respectively. Figure 19 presents the earthquake damage and presents a maximum percentage of complete damage of maximum 30% per census block in a large affected area. In contrast, Fig. 20 presents the tsunami damage and presents a maximum percentage of complete damage going until 100% per census block; however, a smaller area is affected. Figure 19 and Fig. 20 focus on the difference of damages when considering only a tsunami or a combined earthquake and tsunami event. Certain areas on the coast of Trinity, affected by only tsunamis, are in a more important category of damage when considering a combined earthquake and tsunami event. The most impressive change is the larger impacted area in the centre of Trinity, due to fact that the buildings already damaged by the earthquake are

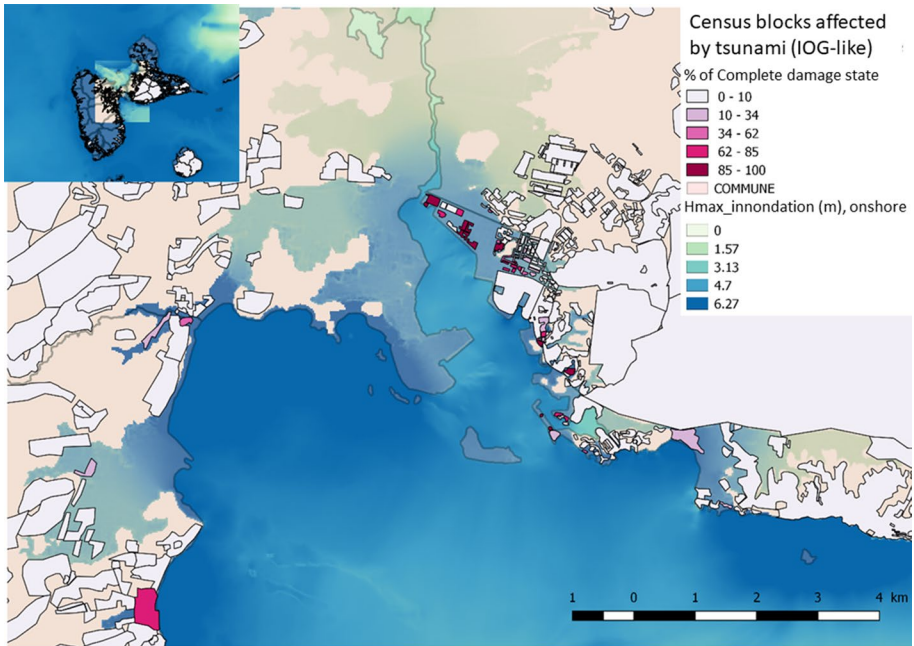


Fig. 14 Guadeloupe tsunami, IOG-like event (inspired from 1843 earthquake), zoomed in on Pointe-à-Pitre Bay: percentage of complete damage state per census block

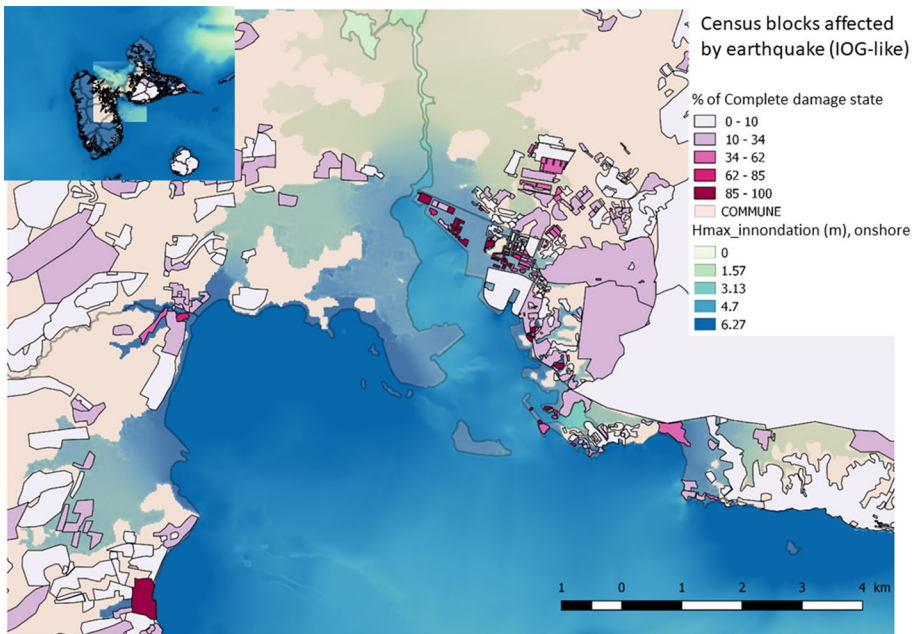


Fig. 15 Guadeloupe earthquake, IOG-like event (inspired from 1843 earthquake), zoomed in on Pointe-à-Pitre Bay: percentage of complete damage state per census block

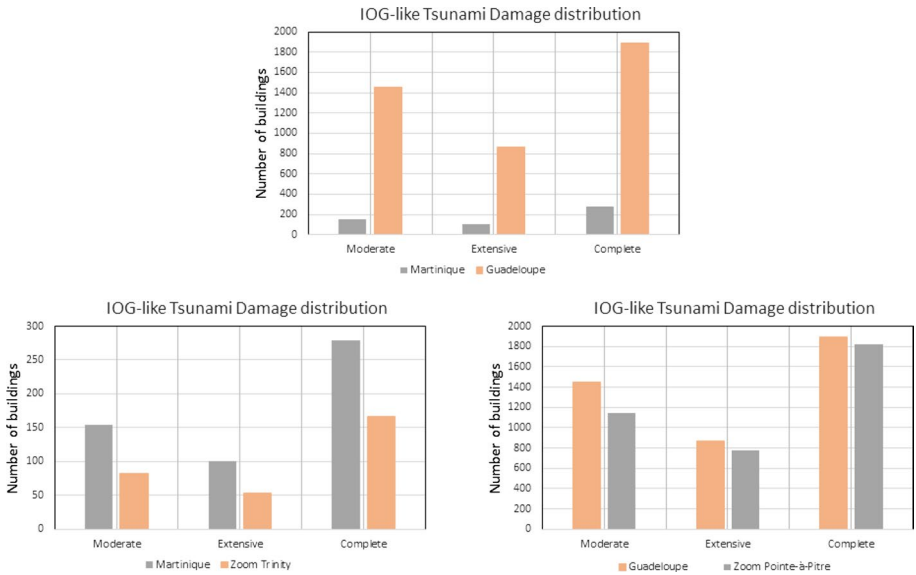


Fig. 16 Damage distributions for the IOG-like tsunami (inspired from 1843 earthquake)

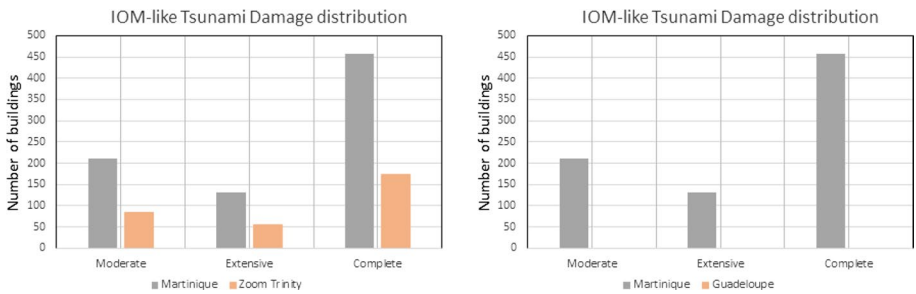


Fig. 17 Damage distributions for the IOM-like tsunami (inspired from 1839 earthquake)

more impacted by the tsunami when considering the previous damages (Fig. 21) than when these damages are not considered (Fig. 20).

6 Discussion

Tables 4 and 5 present the damage results for Martinique and Guadeloupe, respectively, for the IOG-like and IOM-like earthquakes and for the three phenomena sequence approaches: earthquake only, tsunami only and combined cascade events earthquake and tsunami. The earthquake damages are expressed in terms of damage degrees, from D0 to D5, and the tsunami and combined event damages are expressed in terms of Slight, Moderate, Extensive and Complete. Table 3 makes the connection between the definition of damage levels following different methodologies. However, the damage state classification is a complicated

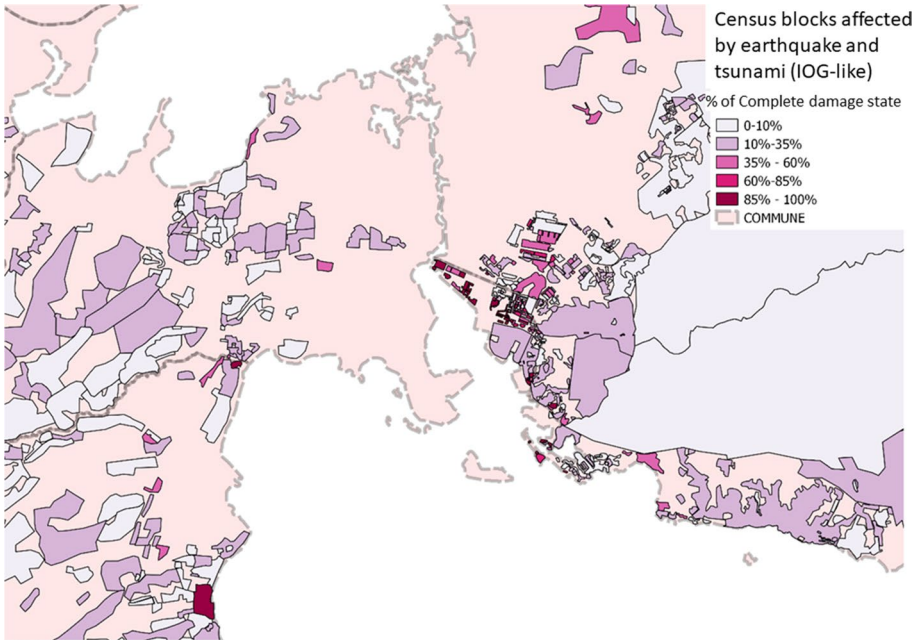


Fig. 18 Guadeloupe combined earthquake and tsunami, IOG-like event (inspired from 1843 earthquake), zoomed in on Pointe-à-Pitre Bay: percentage of complete damage state per census block

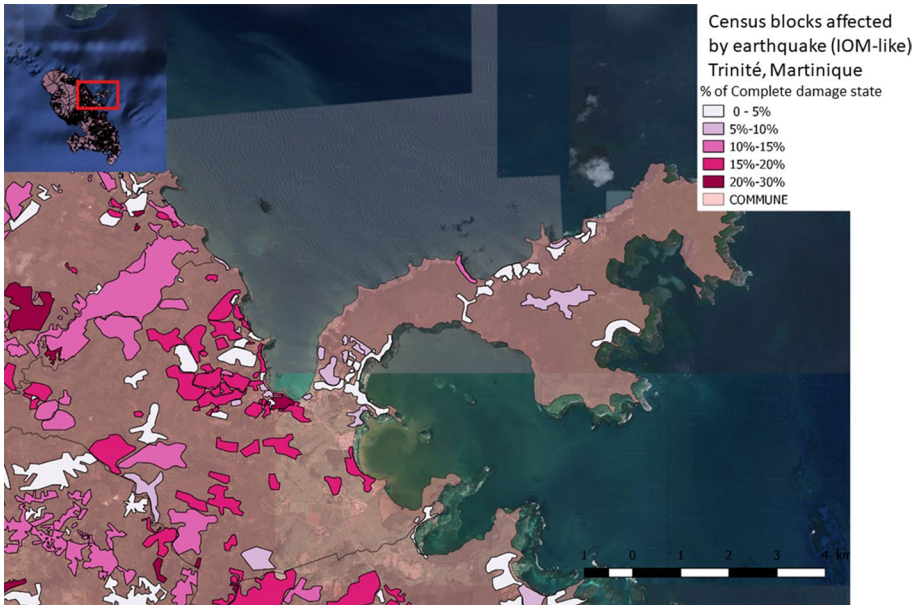


Fig. 19 Martinique IOM-like (inspired from 1839 earthquake) earthquake damage, zoom on Trinité: percentage of complete damage state per census block

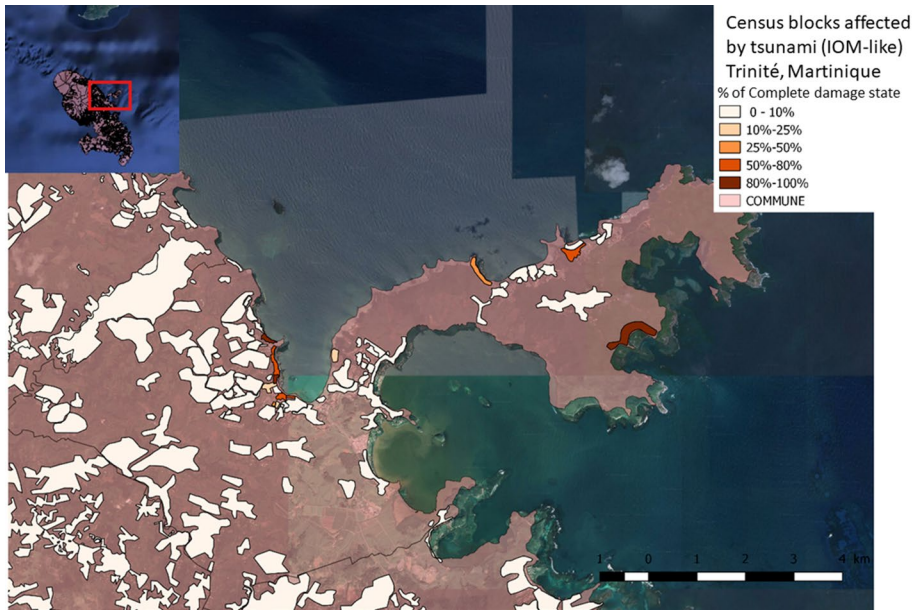


Fig. 20 Martinique IOM-like (inspired from 1839 earthquake) tsunami damage, zoom on Trinité: percentage of complete damage state per census block

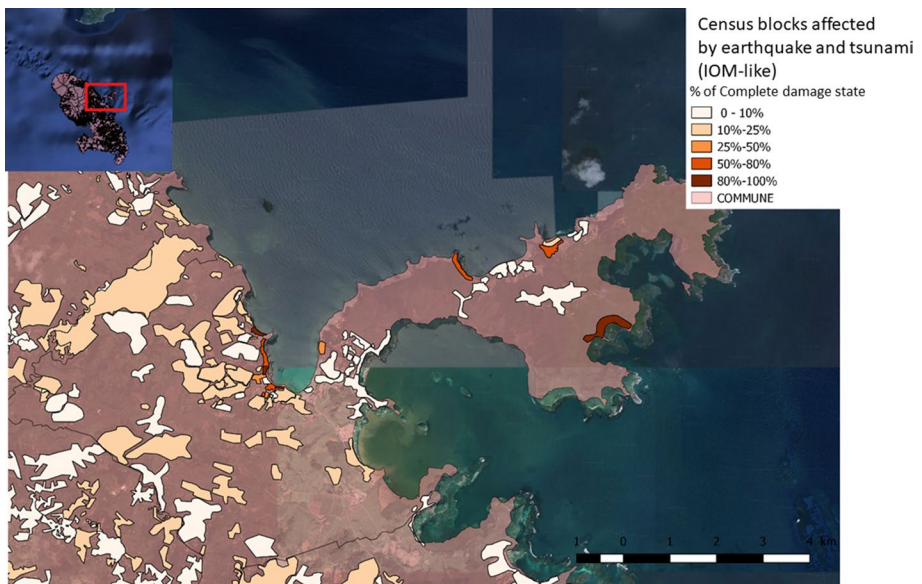


Fig. 21 Martinique IOM-like (inspired from 1839 earthquake) cascade earthquake–tsunami damage, zoom on Trinité: percentage of complete damage state per census block

and tricky issue that can have a big impact on the results. As discussed in Introduction and in Chapter 4.2, we make some hypotheses of the damage states, but future studies done by other researchers for better characterization, and connection between the damage states, can be easily adopted in our methodology. As the estimation of damages is based on a statistical methodology, the numbers in Tables 4 and 5 are rounded to the nearest decimal.

In Martinique, we inventoried a total number of 2950 census blocks that cover the entire island. For this total number of census blocks, only 97 areas are affected by the tsunami induced by an event IOM-like earthquake and only 74 for a tsunami induced by IOG-like earthquake. The affected percentage of census block is around 3%, but the extensive and complete damages increasing much more, arriving until almost doubling in certain combination of event and exposed territory. The same range of values, related to the contrast between the small territory affected by the tsunami and the high increasing of damages for the combined event, are observed for the Guadeloupe Island. For a tsunami induced by IOG-like earthquake, 150 census blocks are impacted on a total of 2054 census blocs. However, the hypotheses used for a tsunami induced by IOM-like earthquake affect only 6 census blocks in Guadeloupe. This is a very insignificant number and is completely in the error range of the methodology; hence, the zoom in Guadeloupe on IOM-like event is not presented in Table 5.

When we study the occurrence of two natural phenomenon, a tricky issue is to evaluate the temporality as well as the spatiality of the two events. As described above, the area affected by the tsunami is, of course, the costal territory, and it is comparatively much smaller than the area affected by the ground motion. The first issue is to correctly identify the area, and the exposed elements affected by the two events. The correct estimation of this area, and of the number of the affected elements, is essential for a good application of the relations used to combine the damages coming from the both events and can reduce the bias on the results. To quantify the effect of the increasing of the vulnerability due to the damages of the first event, we compare the damage results only in the areas affected by the tsunami, since they are a subject of the vulnerability changes. Table 6, and Figs. 22 and 24 present the results only for the area affected by the tsunami. Further, on this paper, we are paying a particular interest to the differences of the results expressed in damaged buildings in this area, due to the different applied approaches.

Contrary to IOM-like tsunami, the IOG-like tsunami, for which the epicentre is situated in offshore of Guadeloupe, affects the both islands. In Martinique, the damages caused only by tsunami are not so different from the damages caused by tsunami and earthquake combined events (Fig. 22, left). This can have two explanations: either the water height is shallow, hence there is not a sur-damage due to tsunami event, or the earthquake did not damaged the structures, and hence, the combined event can be assimilated to an only tsunami event (the only event that has a sufficient intensity to provoke damages).

In order to help to discriminate between the two possibilities mentioned above, we are plotting, in Fig. 23, the moment flux values as a function of the probability of exceedance of a certain damage degree. It can be notice that the maximum MMF for IOG is in the range of $25 \text{ m}^*(\text{m/s})^2$ and around $40 \text{ m}^*(\text{m/s})^2$ for IOM. For IOG, the damage state the most impacted is the Moderate State for a value of MMF beneath $10 \text{ m}^*(\text{m/s})^2$, while for IOM the three damage states are impacted by the manner and order of treating the events (Moderate, Extensive and Complete). The inversion of the probabilities, between the tsunamis only event and cascade events earthquake and tsunamis, is more apparent for the IOM. For IOM, in between the range from 20 to $30 \text{ m}^*(\text{m/s})^2$ we have systematically higher percentage of tsunami damages in Moderate state and, in consequence, higher percentage of damage for the Complete damage state, due to conjoint events, tsunami and earthquake.

Table 4 Damage results for Martinique Island for IOG-like and IOM-like earthquake and three phenomena approaches: earthquake, tsunami and cascade earthquake and tsunami

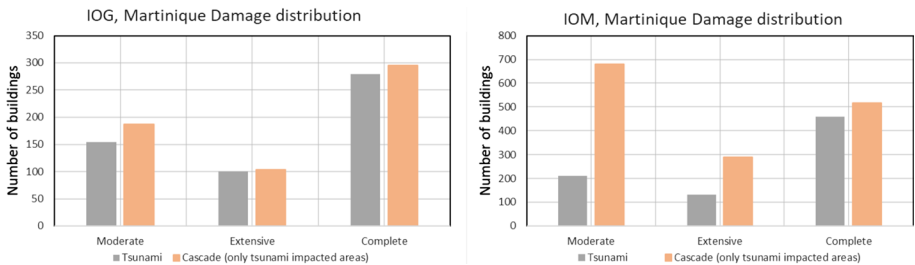
Territory	Event	Earthquake damages							Tsunami damages				Cascade event earthquake and tsunami damages			
		D0	D1	D2	D3	D4	D5	S	M	E	C	S	M	E	C	
Martinique	IOG	77,840	35,910	13,750	3570	520	20	131,080	150	100	280	130,330	320	140	820	
	IOM	23,340	36,190	36,710	24,660	9490	1210	130,810	210	130	460	118,790	1040	640	11,140	
Zoom Trinity	IOG	3000	1240	450	110	10	0	4520	80	50	170	4480	90	60	180	
	IOM	980	1340	1300	850	310	40	4500	90	60	170	4090	120	100	520	

Table 5 Damage results for Guadeloupe Island for IOG-like and IOM-like earthquake and three phenomena approaches: earthquake, tsunami and cascade earthquake and tsunami

Territory	Event	Earthquake damages					Tsunami damages					Cascade event earthquake and tsunami damages				
		D0	D1	D2	D3	D4	D5	S	M	E	C	S	M	E	C	
Guadeloupe	IOG	18,370	41,950	51,120	39,250	18,240	3640	168,350	1450	870	1890	144,660	2240	2460	23,210	
	IOM	138,650	26,200	6410	1170	120	0	172,560	0	0	0	171,260	1180	0	120	
Zoom Pointe-à-Pitre	IOG	180	590	1150	1540	1270	460	1450	1140	780	1820	320	760	1120	3010	

Table 6 Martinique and Guadeloupe comparison of damage only by the area affected by tsunami

Territory	Event	Tsunami damages				Cascade event earthquake and tsunami damages			
		S	M	E	C	S	M	E	C
Martinique	IOG	131,080	150	100	280	131,020	190	100	290
	IOM	130,810	210	130	460	130,120	680	290	520
Guadeloupe	IOG	168,350	1450	870	1890	165,330	2560	1730	2940

**Fig. 22** Damage distributions for IOG-like (inspired from 1843 event) and IOM-like (inspired from 1839 event) tsunamis in Martinique, for tsunami event and cascade earthquake and tsunami event (representation of damages only in the areas impacted by tsunami)

This gives some numerical range of value and confirms the visual observation from the comparison of Figs. 19, 20 and 21.

In Guadeloupe, the damages coming from the combined events are much more important than the damages coming only from tsunami event (Fig. 24). These should be associated with Figs. 14, 15 and 18, which localize, at the scale of the census block, the range of percentage of damages coming from different sequences of physical events and with Fig. 25 which presents the moment flux values as a function of the probability of exceedance of a certain damage degree, in Guadeloupe.

Using the damage results obtained from separate calculation coming from earthquake and coming from tsunami, we calculated the probabilities of damage to the structures due to the combine earthquake and tsunami hazards using HAZUS (2017) formulas from 5.18 to 5.21. These probabilities of damage from combined hazards calculated using HAZUS formulations are compared with the values calculated numerically in this study for the cascade event simulation, with the degradation of the vulnerability of the exposed elements affected by the first event. The comparison between the probabilities of damage to the structures using HAZUS and this study is presented in Figs. 26 and 27 for Trinite, the zoomed area of Martinique for IOM and, respectively, IOG events.

We can observe that in our study the probabilities of being in Complete damage state are systematically superior to the same probabilities calculated with the HAZUS Formulas. For the Extensive damage state, our study gives less probabilities that the HAZUS Formulas. The results for Slight and Moderate damage states are not so different between the two approaches, which means that the reduction in the capacity curves do not affect significantly these damage states. Also, the equivalence of the damage scales (Table 3) can induce a bias to this issue for the lower damage state (Slight and Moderate), but this was discussed previously. We can also see that the more the earthquake event is damageable

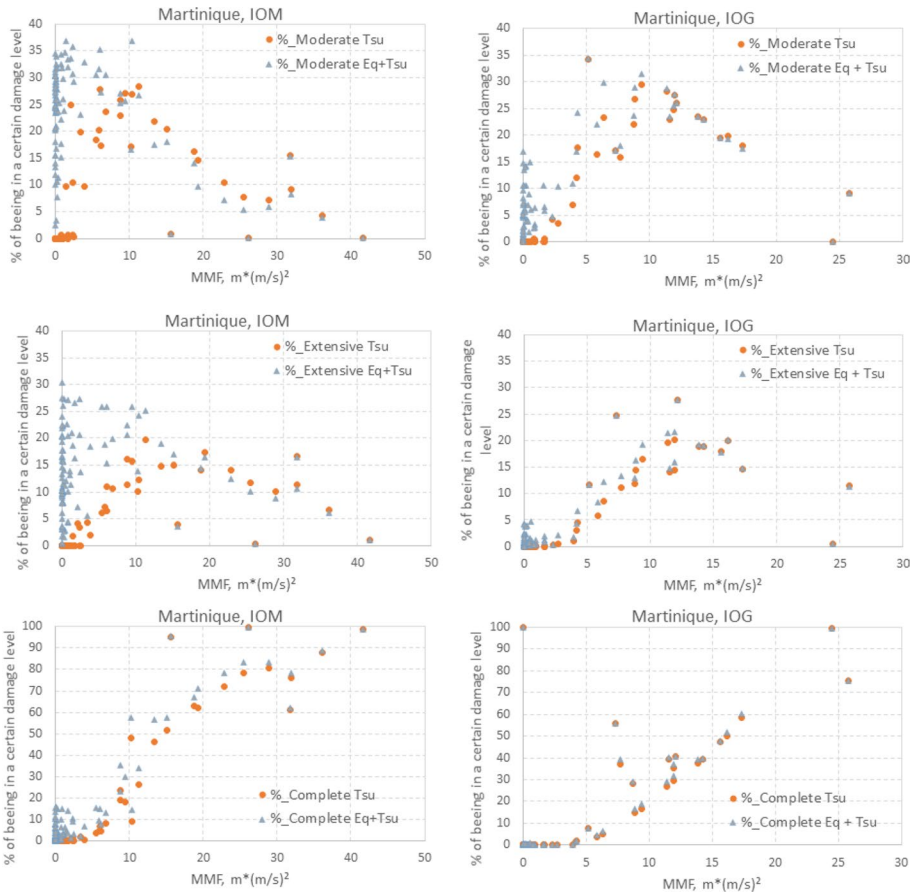
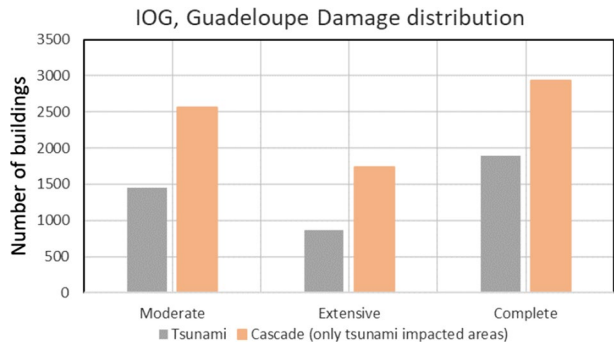


Fig. 23 Relation between the moment flux ($h \cdot v^2$) and the Damage States (Moderate, Extensive, and Complete) calculated for tsunami event and for combined tsunami and earthquake events, for Martinique Island

Fig. 24 Damage distributions for IOG-like tsunami in Guadeloupe, for tsunami event and cascade earthquake and tsunami event (representation of damages only in the areas impacted by tsunami). No tsunami damages for IOM-like event



(before the impact of the tsunami), the more the differences of the results coming from the two approaches are higher. In Fig. 26, for IOM event, the Complete damage state for HAZUS approach is equal to 5%, and in our study, the Complete damage state is around 13%. This difference is vanishing in Fig. 27, IOG event, where of the both approaches the Complete damage state is around 10%. In both situations, we remember that you are treating the same territory with the same approaches, and only the characteristic of the seismic event are changing. In both cases, the tsunami event is almost the same damageable, but for IOM case, the earthquake damage is more important than for the IOG event, which may cause the differences in the combined results. This observation is also verifiable in the case of Guadeloupe (Fig. 28), where the damages from earthquake event are important and the difference in the Complete damage state from the both approaches is of around 10%.

As discussed in the previous sections, the combination of the damages coming from a tsunami and earthquake is quite complicated, since the scale of the impacted area and the damage description are not of the same order. Some formulas for combining the results from the separated hazard calculations are proposed in the literature; however, the results obtained in this paper show that the number of damages is closely related to a specific area, its topography, cartography and its building physical characteristics, and it can be very difficult to generalize this combination formula to others areas. Moreover, for the same affected area, but different characteristics of the seismic event, and hence of the tsunami impact, the combination of the results can be difficult. This is the case for the Trinité area affected by IOM and IOG events. For the IOM event, the results between the two approaches are quite similar, while for the IOG event, in exactly the same area, the results show significant differences especially for the Complete damage state. In addition, in our study, we can notice that the amount of important damages caused by the earthquake event, may be the cause of the differences between the results, but this should be confirmed by more studies in other geographic areas.

7 Conclusions

The relationship between the number of damaged structures and earthquakes alone and earthquake-and-tsunami cascade events was investigated in this paper from informatics, practical and realistic viewpoints. The database for buildings and soil responses are based on field investigation campaigns performed during several projects funded by the French Government. Several practical novelties are applied to the combined earthquake–tsunami damage scenario. First, the acquisition of each intensity measure for all the time of the event is primordial, since the maximum sea surface elevation and the maximum water velocity are not necessary in the same time in the same spatial cells. Hence, this information allows us to stick as close to the phenomenon as possible, instead of using median values of the intensity measure parameters. Second, for the cascade scenario, we considered the degradation of the initial vulnerability of a damaged structure, expressed here by a capacity curve for tsunami calculation, considering the reached limit state by the structure after the first event (i.e. the earthquake). This step complicates the direct hazard–vulnerability–damage calculation, since the exposed elements are updated in the number of structures but also consider the new degraded vulnerability, which implies an informatics loop and a multiplication of the vulnerability characteristic equal to the number of the damage degree used to describe the first event. From a general point of view, this procedure can be applied to other areas of study but also to the other combinations of the two natural

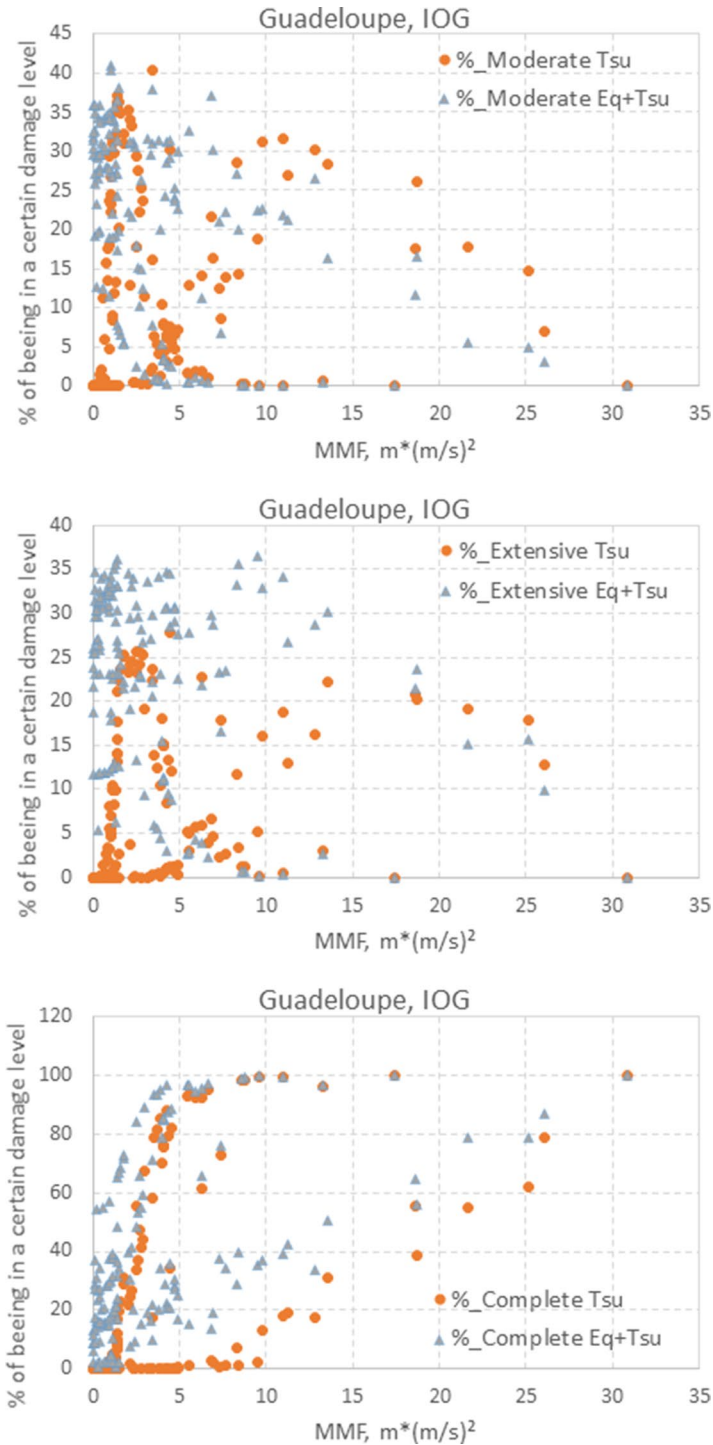


Fig. 25 Relation between the moment flux (H^*v^2) and the Damage States (Moderate, Extensive, and Complete) calculated for tsunami event and for combined tsunami and earthquake events, for Guadeloupe Island

Damage probabilities for the IOM event in Martinique (Trinité):
eq, tsunami, combined probabilities - this study and HAZUS

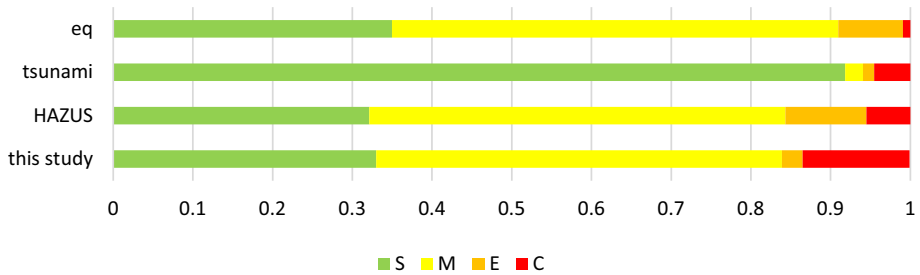


Fig. 26 Damage probabilities for the IOM event in Trinité for Slight (S), Moderate (M), Extensive (E) and Complete (C) damage states resulting from (i) earthquake event, (ii) tsunami event, (iii) HAZUS approach for combining the damages coming from earthquake and tsunami and (iv) this study approach for combining the damages coming from earthquake and tsunami

Damage probabilities for the IOG event in Martinique (Trinité):
eq, tsunami, combined probabilities - this study and HAZUS

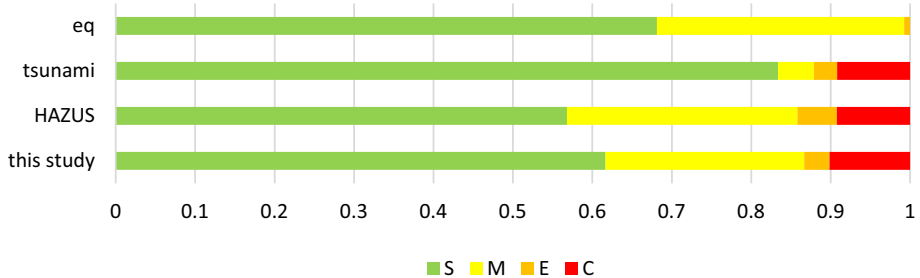


Fig. 27 Damage probabilities for the IOG event in Trinité for Slight (S), Moderate (M), Extensive (E) and Complete (C) damage states resulting from (i) earthquake event, (ii) tsunami event, (iii) HAZUS approach for combining the damages coming from earthquake and tsunami and (iv) this study approach for combining the damages coming from earthquake and tsunami

phenomena. This step has the merit of overcoming a complicated stage of the combination of damage coming from two different hazards, as is currently used. From a specific point of view, the combined scenario provides an opportunity to observe real damages and to quantify them stemming from three different approaches: earthquake only, tsunami only and combined earthquake and tsunami event. This quantified result highlights the complexity of treating two phenomena that have a difference in their scale of impact and of intensity of damage: a large area of impact for an earthquake, and graduating damage and a considerably more localized area of impact for a tsunami, but heavy damages. However, the correspondences between the RISK-UE and the HAZUS typologies (Table 2) and between the RISK-UE and the HAZUS damage degrees (Table 3) are based on experts choice and these can introduce some biases in the results, but even with others choice of the correspondence between these two parameters, the calculation method remains reproducible and stable. Future work will focus on a better integration of the tsunami flooding in the damaged area (up to high-resolution modelling) including an update of the Manning coefficient during

Damage probabilities for the IOG event in Guadeloupe (PàP): eq, tsunami, combined probabilities - this study and HAZUS

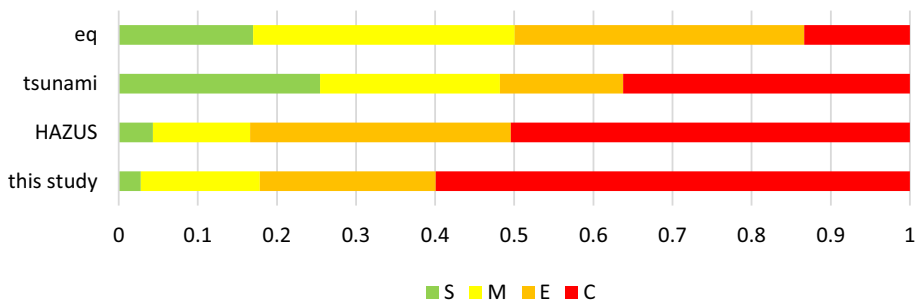


Fig. 28 Damage probabilities for the IOM event in Guadeloupe, Pointe-a-Pitre (PàP) for Slight (S), Moderate (M), Extensive (E) and Complete (C) damage states resulting from (i) earthquake event, (ii) tsunami event, (iii) HAZUS approach for combining the damages coming from earthquake and tsunami and (iv) this study approach for combining the damages coming from earthquake *and tsunami*

damage calculation. Another important issue to be addressed in the future studies is the influence of the debris of the collapsed buildings on the force applied to the structure but also on the changing of manning roughness coefficient due to the debris.

Acknowledgements This article was supported by: (i) an internal BRGM research programme (VULNERISK/MULTIRISK / Platform 2017 and 2018), (ii) a project on tsunami hazard evaluation in Martinique supported by regional Institution (Le Roy et al. 2017) and (iii) the project TANDEM (Tsunamis in the Atlantic and the English ChaNnel; Definition of the Effects through numerical Modeling, 2014–2018) funded by the ANR (French National Research Agency). We thank the National Institutions for support during the 2007 to 2013 field studies investigation in the French West Indies (programme “Plan Seisme Antilles”). We thank Myriam Belvaux, Didier Bertil, Aude Nachbaur, Legendre Yoann and Valérie Clouard for useful discussions on various aspects of this study. We would like to thank to the internal BRGM research project, who since our study, implement the methodology into the VIGIRISKS platform (<https://gitlab.brgm.fr/brgm/vigirisks/communities/end-users>).

Open Access This article is licensed under a Creative Commons Attribution 4.0 International License, which permits use, sharing, adaptation, distribution and reproduction in any medium or format, as long as you give appropriate credit to the original author(s) and the source, provide a link to the Creative Commons licence, and indicate if changes were made. The images or other third party material in this article are included in the article’s Creative Commons licence, unless indicated otherwise in a credit line to the material. If material is not included in the article’s Creative Commons licence and your intended use is not permitted by statutory regulation or exceeds the permitted use, you will need to obtain permission directly from the copyright holder. To view a copy of this licence, visit <http://creativecommons.org/licenses/by/4.0/>.

References

- Amakuni K, Terazono N (2011) Basic analysis on building damages by tsunami due to the 2011 Great East Japan earthquake disaster using. In: 15 world conference on earthquake engineering. Available at: http://www.iitk.ac.in/nicee/wcee/article/WCEE2012_3628.pdf
- Atkinson GM (2011) Sonley E (2000) Relationships between modified Mercalli intensity and response spectra. Bull Seismol Soc Am 90:537–544B10308. <https://doi.org/10.1029/2011JB008443>
- Attary N, Unnikrishnan VU, van de Lindt JW, Cox DT, Barbosa AR (2017) Performance-based tsunami engineering methodology for risk assessment of structures. Eng Struct 141:676–686. <https://doi.org/10.1016/j.engstruct.2017.03.071>

- Belvaux M, Monfort-Climent D, Bertil D, Roullé A, Noury G (2013) Cartographie departementale du risque sismique en Martinique. Openfile BRGM report RP-61904-FR (in French).
- Bertil D, Roule A, Mompelat JM, Auclair S, Bayle E, Bengoubou Valerius M, Bitri A, Chauvet M, Gehl P, Imbault M, Negulescu C, Samyn K, Vanoudheusden E, Vermeersch F (2009) Microzonage sismique des communes de Baie-Mahault et Lamentin (Guadeloupe). Rapport final. Rapport n° 57487.
- Bertil D, Bengoubou-Valérius M, Péricat J, Auclair S (2009) Scénarios Départementaux de Risque Sismique en Guadeloupe. Technical report BRGM/RP-57488-FR. (in French).
- Bernard P, Lambert J (1988) Subduction and seismic hazard in the northern Lesser Antilles arc: revision of the historical seismicity. *Bull Seism Soc Am* 78:1965–1983
- Boutaraa Z, Negulescu C, Arab A et al (2018) Buildings vulnerability assessment and damage seismic scenarios at urban scale: application to Chlef City (Algeria). *KSCE J Civ Eng* 22:3948–3960. <https://doi.org/10.1007/s12205-018-0961-2>
- BRGM, French geological survey, SISFRANCE: SisFrance website for historical earthquakes in the Antilles and the Caribbean region, available at: www.sisfrance.net/Antilles (last access: 2018), 2009; and Official website for historical tsunamis in France, available at: www.tsunamis.fr (last access: 2018), 2010.
- Browning J, Thomas N (2016) An assessment of the tsunami risk in Muscat and Salalah Oman, based on estimations of probable maximum loss. *Int J Disaster Risk Reduct* 16:75–87. <https://doi.org/10.1016/j.ijdr.2016.02.002>
- Briggs RW, Sieh K, Meltzner AJ, Natawidjaja D, Galetzka J, Bambang S, Hsu Y-j, Simons M, Hananto N, Suprihanto I, Prayudi D, Avouac J-P, Prawirodirdjo L, Bock Y (2006) Deformation and slip along the sunda megathrust in the great 2005 nias-simeulue earthquake. *Science* 311(5769):1897–1901. <https://doi.org/10.1126/science.1122602>
- Charvet I, Macabuag J, Rossetto T (2017) Estimating tsunami-induced building damage through fragility functions: critical review and research needs. *Front Built Environ* 3:36. <https://doi.org/10.3389/fbuil.2017.00036>
- Crowley H, Colombi M, Crempien J, Erduran E, Lopez M, Liu H, Mayfield M, Milanesi M (2010a) GEM1, Seismic Risk Report: Part 1, GEM Technical Report 2010–5. GEM Foundation, Pavia
- Crowley H, Cerisara A, Jaiswal K, Keller N, Luco N, Pagani M, Porter K, Silva V, Wald D, Wyss B (2010b) GEM1, Seismic Risk Report: Part 2, GEM Technical Report 2010–5. GEM Foundation, Pavia
- DeMets C, Jansma PE, Mattioli GS, Dixon TH, Farina F, Bilham R, Calais E, Mann P (2000) GPS geodetic constraints on Caribbean–North America plate motion. *Geophys Res Lett* 27:437–440
- Douglas J, Climent DM, Negulescu C, Roullé A, Sedan O (2015) Limits on the potential accuracy of earthquake risk evaluations using the L’Aquila (Italy) earthquake as an example. *Ann Geophys* 58:1–17
- Eguchi RT, Eguchi MT, Bouabid J, Koshimura S, Graf WP (2013) “HAZUS Tsunami Benchmarking, Validation and Calibration.” Prepared for the Federal Emergency Management Agency through a contract with the Atkins, March 11, 2013
- Epstein W (2011) A probabilistic risk assessment practioner looks at the great east japan earthquake and tsunami. A Ninokata Laboratory White Paper, Tokyo Institute of Technology, Ninokata Laboratory. Retrieved from <http://woody.com/wp-content/uploads/2011/06/A-PRA-Practitioner-looks-at-the-Great-East-Japan-Earthquake-and-Tsunami.pdf>
- Federal Emergency Management Agency (FEMA) (1999) HAZUS99 earthquake loss estimation methodology, User Manual. Federal Emergency Management Agency, Washington, D.C.
- Federal Emergency Management Agency (FEMA) (2004) Using HAZUS-MH for Risk Assessment (FEMA 433). Report of the Federal Emergency Management Agency, Washington, D.C.
- Feuillet N, Beauducel F, Tapponnier P (2011) Tectonic context of moderate to large historical earthquakes in the Lesser Antilles and mechanical coupling with volcanoes. *J Geophys Res* 116:B10308. <https://doi.org/10.1029/2011JB008443>
- Federal Emergency Management Agency (FEMA) (2011) Hazus-MH—MH 2.0 earthquake model technical manual. FEMA, Mitigation Division, Washington, DC, Unites States. Accessed 8 July 2011
- Fraser SA, Power WL, Wang X et al (2014) Tsunami inundation in Napier New Zealand, due to local earthquake sources. *Nat Hazards* 70:415. <https://doi.org/10.1007/s11069-013-0820-x>
- Gasparini P, Garcia-Aristizabal A (2014) Seismic Risk Assessment, Cascading Effects, Encyclopedia of Earthquake. Engineering. https://doi.org/10.1007/978-3-642-36197-5_260-1
- Garcia-Aristizabal A, Bucchignani E, Palazzi E, D’Onofrio D, Gasparini P, Marzocchi W (2015) Analysis of non-stationary climate-related extreme events considering climate-change scenarios: an application for multi-hazard assessment in the Dar Es Salaam region, Tanzania. *Nat Hazards* 75:289–320. <https://doi.org/10.1007/s11069-014-1324-z>
- Giovinazzi S, Lagomarsino S (2004) A macroseismic model for the vulnerability assessment of buildings. In: Proceedings of the 13th world conference on earthquake engineering, Vancouver, Canada

- Grunthal G, Musson RMW, Schwarz J, Stucchi M (1998) EMS-98: European Macroseismic Scale, Centre Européen de Géodynamique et de Sismologie, Luxembourg. EMS
- Hancilar U, Tuzun C, Yenidogan C, Erdik M (2010) ELER software—a new tool for urban earthquake loss assessment. *Nat Hazards Earth Syst Sci* 10:2677–2696
- HAZUS (2017) FEMA 2017. Hazus tsunami model technical guidance for hazus version 4.0, Contract No. HSFE60–17-P-0004
- Hill M, Rossetto T (2008) Comparison of building damage scales and damage descriptions for use in earthquake loss modelling in Europe. *Bull Earthq Eng* 6:335. <https://doi.org/10.1007/s10518-007-9057-y>
- Hough SE (2013) Spatial variability of “Did You Feel It?” intensity data: Insights into sampling biases in historical earthquake intensity distributions. *Bull Seismol Soc Am* 103(5):2767–2781
- Jaimes MA, Reinoso E, Ordaz M, Huerta B, Silva R, Mendoza E, Rodríguez JC (2016) A new approach to probabilistic earthquake-induced tsunami risk assessment. *Ocean Coast Manag* 119:68–75. <https://doi.org/10.1016/j.ocecoaman.2015.10.007>
- Japan Cabinet Office (2013) Residential disaster damage accreditation criteria operational guideline. Available at: <http://www.bousai.go.jp/taisaku/nyou.html>
- Kircher CA, Bouabid J (2014) New Building Damage Functions for Tsunami. In: Proceedings of the 10th National Conference in Earthquake Engineering, Earthquake Engineering Research Institute, Anchorage, AK
- Lambert J, Terrier M (2011) Historical tsunami database for France and its overseas territories. *Nat Hazards Earth Syst Sci* 11:1037–1046. <https://doi.org/10.5194/nhess-11-1037-2011>
- Lestuzzi P, Podestà S, Luchini C et al (2016) Seismic vulnerability assessment at urban scale for two typical Swiss cities using Risk-UE methodology. *Nat Hazards* 84:249–269. <https://doi.org/10.1007/s11069-016-2420-z>
- Le Roy S, Lemoine A, Nachbaur A, Legendre Y, Lambert J, Terrier M (2017) Détermination de la submersion marine liée aux tsunamis en Martinique. Rapport BRGM/RP-66547-FR, 177 p., 105 ill., 7 Ann.
- Litto3D ©IGN-SHOM (2016) <https://www.shom.fr/les-activites/projets/modele-numerique-terre-mer/>
- Luco N, Bazzurro P, Cornell CA (2004) Dynamic versus static computation of the residual capacity of a mainshock-damaged building to withstand an aftershock. In: Proceedings of the 13th World Conference on Earthquake Engineering, Paper 2405, Vancouver
- Macabuag J, Rossetto T (2014) Towards the Development of a Method for Generating Analytical Tsunami Fragility Functions. In: Proceedings of the 2nd European Conference on Earthquake Engineering and Seismology, Istanbul, Aug 2014.
- Mignan A, Scolobig A, Sauron A (2016) Using reasoned imagination to learn about cascading hazards: a pilot study. *Disaster Prev Manag* 25(3):329–344. <https://doi.org/10.1108/DPM-06-2015-0137>
- Milutinovic ZV, Trendafiloski GS (2003) RISK-UE: An advanced approach to earthquake risk scenarios with applications to different European towns. WP4: Vulnerability of current buildings
- Molina S, Lang DH, Lindholm CD (2010) SELENA—an open-source tool for seismic risk and loss assessment using a logic tree computation procedure. *Comput Geosci* 36:257–269
- Macabuag J, Rossetto T, Ioannou I, Suppasri A, Sugawara D, Adriano B, Eames FI, Koshimura S (2016) A proposed methodology for deriving tsunami fragility functions for buildings using optimum intensity measures. *Nat Hazards* 84(2):1257–1285
- Murao O, Nakazato H (2010) Vulnerability functions for buildings based on damage survey data in Sri Lanka after the 2004 Indian Ocean tsunami. In: International conference on sustainable built environment (ICSBE-2010) Kandy, pp 371–378
- Negulescu C, Hohmann A, Tellez-Arenas A, Smai F (2019) A web platform for storing, sharing and executing scientific workflows for Natural Risk Assessment: part 1 – data, approaches and case studies. *Geophys Res Abs* 21:1. <http://search.ebscohost.com/login.aspx?direct=true&db=asx&AN=140482820&lang=fr&site=eds-live>
- Okada Y (1985) Surface deformation due to shear and tensile faults in a half-space. *Bull Seismol Soc Am* 75:1135–1154
- Park H, Cox DT (2016) Probabilistic assessment of near-field tsunami hazards: inundation depth, velocity, momentum flux, arrival time, and duration applied to Seaside. *Oregon* 117:79–96. <https://doi.org/10.1016/j.coastaleng.2016.07.011>
- Park H, Cox DT, Barbosa AR (2017) Comparison of inundation depth and momentum flux based fragilities for probabilistic tsunami damage assessment and uncertainty analysis. *Coast Eng* 122:10–26 **Online publication date: 1-Apr-2017**
- Prieto JA, Journeay M, Acevedo AB, Arbelaez JD, Ulmi M (2018) Development of structural debris flow fragility curves (debris flow buildings resistance) using momentum flux rate as a hazard parameter. *Eng Geol* 239:144–157. <https://doi.org/10.1016/j.enggeo.2018.03.014>

- Poisson B, Garcin M, Pedreros R (2009) The 2004 December 26 Indian Ocean tsunami impact on Sri Lanka: cascade modelling from ocean to city scales. *Geophys J Int* 177(3):1080–1090. <https://doi.org/10.1111/j.1365-246X.2009.04106.x>
- Pitilakis K, Crowley H, Kaynia A (eds) (2014) SYNER-G: systemic seismic vulnerability and risk assessment of complex Urban, Utility, lifeline systems and critical facilities. Springer, Dordrecht
- Petrone C, Rossetto T, Goda K (2017) Fragility assessment of a RC structure under tsunami actions via nonlinear static and dynamic analyses. *Eng Struct* 136(2017):36–53. <https://doi.org/10.1016/j.engstruct.2017.01.013>
- Shi F, Kirby JT, Tehranirad B (2012) Tsunami benchmark results for spherical coordinate version of FUN-WAVE-TVD (Version 1.1)- Center for Applied Coastal Research, Univ. of Delaware, Tech. Rep., 2012b, research Report no. CACR-12–02
- Sedan O, Terrier M, Negulescu C, Winter T, Roulle A, Douglas J, Rohmer J, Bes-De-Berc S, De Martin F, Arnal C, Dewez T, Fontaine M (2008) Scénario départemental de risque sismique- Méthodologie et processus de réalisation. Rapport BRGM/RP-55415-FR, 459p.
- Sedan O, Negulescu C, Terrier M, Roulle A, Winter T, Bertil D (2013) Armagedom—a tool for seismic risk assessment illustrated with applications. *J Earthq Eng* 17(2):253–281
- Suppasri A, Charvet I, Imai K, Imamura F (2015) Fragility curves based on data from the 2011 Tohoku-Oki tsunami in Ishinomaki City, with discussion of parameters influencing building damage. *Earthq Spectra*; May 2015 31(2):841–868
- Suppasri A, Mas E, Koshimura S, Imai K, Harada K, Imamura F (2012) Developing tsunami fragility curves from the surveyed data of the 2011 Great East Japan Tsunami In Sendai And Ishinomaki Plains. *Coast Eng J* 54(01):1250008
- Rehman K, Cho Y-S (2016) Building damage assessment using scenario based tsunami numerical analysis and fragility curves. *Water* 8(3):109. <https://doi.org/10.3390/w8030109>
- Ruangrassamee A, Yanagisawa H, Foytong P, Lukkunaprasit P, Koshimura S, Imamura F (2006) Investigation of tsunami-induced damage and fragility of buildings in Thailand after the december 2004 Indian ocean tsunami. *Earthq Spectra* 22:377–401
- Rossetto T, Peiris N, Pomonis A, Wilkinson SM, Del Re D, Koo R, Gallocher S (2007) The Indian ocean tsunami of december 26, 2004: observations in Sri Lanka and Thailand. *Nat Hazards* 42:105. <https://doi.org/10.1007/s11069-006-9064-3>
- RISK-UE: “An advanced approach to earthquake risk scenarios, with applications to different European cities” (2001–2004). Website: <https://www.risk-ue.net>
- Römer H, Willroth P, Kaiser G, Vafeidis AT, Ludwig R et al (2012) Potential of remote sensing techniques for tsunami hazard and vulnerability analysis—a case study from Phang-Nga province, Thailand. *Nat Hazards Earth Syst Sci* 12:2103–2126. <https://doi.org/10.5194/nhess-12-2103-2012>
- Roulle A, Negulescu C, Montfort Climent D, Vanoudheusden E, Barras AV, Auclair S, Samyn K, Imbault M, Vanoudheusden L (2010) Microzonage sismique de la commune de Trinité (Martinique). Rapport final. Rapport n°57664
- Tarbotton C, Dall’Osso F, Dominey-Howes D, Goff J (2015) The use of empirical vulnerability functions to assess the response of buildings to tsunami impact: comparative review and summary of best practice. *Earth Sci Rev* 142:120–134. <https://doi.org/10.1016/j.earscirev.2015.01.002>
- Tellez-Arenas A, Hohmann A, Quentin A, Negulescu C, Smaï F (2019) A web platform for storing, sharing and executing scientific workflows for Natural Risk Assessment: part 2 - description of an interoperable architecture based on open-source components. *Geophys Res Abs* 21:1
- Weatherall P, Marks KM, Jakobsson M, Schmitt T, Tani S, Arndt JE, Rovere M, Chayes D, Ferrini V, Wigley R (2015) A new digital bathymetric model of the world’s oceans. *Earth Space Sci* 2(8):331–345
- Whitman RV, Reed JW, Hong ST (1974) Earthquake Damage Probability Matrices. In: Proceedings of the 5th ECEE, Rome, pp. 2531
- Vamvatsikos D, Allin Cornell C (2006) Direct estimation of the seismic demand and capacity of oscillators with multi-linear static pushovers through IDA. *Earthq Eng Struct Dyn* 35:1097–1117. <https://doi.org/10.1002/eqe.573>
- Youngs RR, Chiou SJ, Silva WJ, Humphrey JR (1997) Strong ground motion attenuation relationships for subduction zone earthquakes. *Seismol Res Lett* 68(1):58–73
- Yu FJ, Yuan Y, Zhao LD et al (2011) Evaluation of potential hazards from teletsunami in China: tidal observations of a teletsunami generated by the Chile 8.8 M w earthquake. *Chin Sci Bull* 56:1108–1116. <https://doi.org/10.1007/s11434-010-4307-9>
- Zahibo N, Pelinovsky EN (2001) Evaluation of tsunami risk in the Lesser Antilles. *Nat Hazards Earth Syst Sci* 1(4):221–231

Yamazaki Y, Cheung K (2011) Shelf resonance and impact of near-field tsunami generated by the 2010 Chile earthquake. *Geophys. Res. Lett.* <https://doi.org/10.1029/2011GL047508>

Publisher's Note Springer Nature remains neutral with regard to jurisdictional claims in published maps and institutional affiliations.

Affiliations

Caterina Negulescu¹  · Abed Benaïchouche¹ · Anne Lemoine¹ · Sylvestre Le Roy¹ · Rodrigo Pedreros¹

✉ Caterina Negulescu
c.negulescu@brgm.fr

¹ BRGM (French Geological Survey), 3 Avenue Claude Guillemin, 45060 Orléans Cedex 2, France